## A Driving-Style-Adaptive Framework for Vehicle Trajectory Prediction

 $\begin{array}{cccc} \textbf{Di Wen}^{1,2,3} & \textbf{Yu Wang}^2 & \textbf{Zhigang Wu}^{1,3} \\ \textbf{Zhaocheng He}^{1,2,3*} & \textbf{Zhe Wu}^{2,*} & \textbf{Zheng Qingfang}^2 \end{array}$ 

<sup>1</sup>Sun Yat-sen University <sup>2</sup>Pengcheng Laboratory <sup>3</sup>Guangdong Provincial Key Laboratory of Intelligent Transportation System {wend25,wuzhig6}@mail2.sysu.edu.cn hezhch@mail.sysu.edu.cn {wangy12,wuzh02,zhengqf01}@pcl.ac.cn

#### **Abstract**

Vehicle trajectory prediction serves as a critical enabler for autonomous navigation and intelligent transportation systems. While existing approaches predominantly focus on pattern extraction and vehicle-environment interaction modeling, they exhibit a fundamental limitation in addressing trajectory heterogeneity originating from human driving styles. This oversight constrains prediction reliability in complex real-world scenarios. To bridge this gap, we propose the Driving-Style-Adaptive (DSA) framework, which establishes the first systematic integration of heterogeneous driving behaviors into trajectory prediction models. Specifically, our framework employs a set of basis functions tailored to each driving style to approximate the trajectory patterns. By dynamically combining and adaptively adjusting the degree of these basis functions, DSA not only enhances prediction accuracy but also provides **explanations** insights into the prediction process. Extensive experiments on public real-world datasets demonstrate that the DSA framework outperforms state-of-the-art methods.

#### 1 Introduction

Vehicle Trajectory Prediction (VTP) serves as a fundamental capability for numerous intelligent transportation applications, including autonomous driving systems [1, 2, 3], motion planning algorithms [4, 5] and adaptive traffic control frameworks [6, 7]. Recent advances in VTP achieve notable progress through two primary paradigms: (1) capturing temporal patterns from historical trajectories and modeling vehicle interactions [8, 9, 10, 11], and (2) leveraging structured scene representations that incorporate road topology and regulatory constraints [12, 13, 14, 15]. However, these methods often overlook the originator of the trajectory: human drivers [16, 17], whose diverse behavior leads to heterogeneous trajectory patterns.

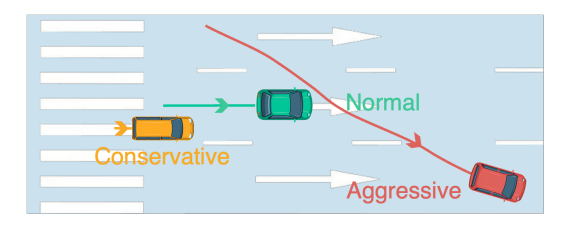


Figure 1: Illustration of three driving styles: Conservative drivers typically move slowly or stop to avoid obstacles; Aggressive drivers often travel at high speeds and are prone to overtaking other vehicles; Normal drivers maintain a constant speed and frequently change lanes to ensure safety.

In this paper, we propose an **adaptive** VTP framework based on distinct **driving styles** [18, 19]: Conservative, Aggressive and Normal (CAN). Each driving style manifests in characteristic trajectory

<sup>\*</sup>Joint Corresponding Authors.

patterns, as illustrated in Figure 1. limited variability (conservative), non-smooth trajectories (aggressive) and frequent yet smooth motion changes (normal). For each styles, we employs variable basis functions within Kolmogorov-Arnold Networks (KANs) [20] to capture these trajectory patterns. In complex real-world scenarios, driver behavior often reflects a probabilistic mixture of weighted driving styles [21].

Our framework comprises two core components: (1) the matching between driving styles and their corresponding basis functions, and (2) the weighted combination and adjustment of the degrees of these functions. Additionally, inspired by the Weierstrass Approximation Theorem [22], our proposed DSA framework extends KANs from a theoretical perspective. Each matching in (1) is further grounded in the mechanical properties of basis functions, thereby providing explanations for our DSA framework.

Our main contributions in this paper are summarized as follows:

- To address the vehicle trajectory prediction task, we propose for the first time, a novel Driving-Style-Adaptive (DSA) framework tailored to the **driving styles** of human drivers and effectively leverages trajectory information.
- We utilize polynomial approximation operators to approximate and predict trajectories under different driving styles: Conservative, Aggressive and Normal (CAN). These operators support a mathematical explanation matching mechanism that matches each driving style with a corresponding polynomial form.
- The experimental results on real-world datasets (nuScenes, Argoverse and Waymo) demonstrate that our model significantly outperforms existing methods in vehicle trajectory prediction.

#### 2 Preliminary & Related Work

#### 2.1 Task Definition: Vehicle Trajectory Prediction (VTP)

VTP aims to predict the future trajectory of vehicles based on history trajectory or other informations available in a given scenario. In recent years, deep learning based VTP methods are categorized into two groups [23]: (i) knowledge-based methods, which incorporate specific information such as maps [24, 25], vehicles [9, 26] and interactions [27, 28] to represent the environment or vehicle behaviour. (ii) knowledge-free methods, which rely on deep learning's ability to encode complex data features, modeling them using structures such as tensors [29, 30] or attention mechanisms [31, 32].

Following above works, we analyze traffic scenes involving N vehicles (agents). The trajectory of each vehicle i in historical interval [0,T] is denoted as  $X_i = \left\{s_i^{-t}, \cdots, s_i^0\right\}$ . Each state  $s_i^\star$  is a 5-dimensional vector representing the (x,y) position, velocity, acceleration, and the nearest lane segments ID. The superscript  $\star$  denotes the time step. Similarly, the future trajectory in interval [0,T] is given by  $Y_i = \left\{s_i^0, \cdots, s_i^T\right\}$ .

#### 2.2 Basic Network: Kolmogorov-Arnold Networks (KANs)

KANs [20] are inspired by the mathematical principles [33, 34, 35] of the Kolmogorov-Arnold representation theorem [36, 37, 38], stated as follows:

**Theorem 2.1** (Kolmogorov-Arnold representation Theorem) For any multivariate continuous function  $f:[0,1]^n \to \mathbb{R}$ , f can be represented as a finite composition of univariate continuous functions  $\phi_{ij}:[0,1]\to\mathbb{R}$  and  $\Phi_j:\mathbb{R}\to\mathbb{R}$ , with the binary operation of addition such that:

$$F = f(x_1, \dots, x_n) = \sum_{j=1}^{2n+1} \Phi_j \left[ \sum_{i=1}^n \phi_{ij}(x_i) \right].$$
 (1)

The key innovation of KANs lies in implementing the residual activation functions  $\phi(x)$  in Equation (1) as:

$$\phi(x) = w_b b(x) + w_s \psi(x), \tag{2}$$

where b(x) = silu(x) and  $\psi(x) = \text{spline}(x)$ . Unlike Multi-Layer Perceptrons (MLPs [39, 40]), which utilize fixed activation functions associated with nodes ("neurons"), KANs feature learnable

 $\phi(x)$  on edges ("weights"). However, due to the inherent complexity of these functions, the speed and scalability of the original KANs are not satisfactory [41]. Consequently, a variety of KAN-based applications are emerged in AI4Science tasks [42, 43, 44, 45, 46, 47]. To the best of our knowledge, we are the first to extension KANs to the VTP task. We achieve this by expanding the set of basis functions  $\psi(x)$  to match different driving styles and by grounding this matching in both mathematical theory and task-specific behavior.

#### 2.3 Core Theory: Applying Polynomials as Basis Functions

As describe in Section 2.2, a fixed basis function has inherent limitations. In the VTP task, such a function may fail to adequately approximate diverse trajectory or lane curves. This raises an important question: how can we legitimately expand the class of basis functions? In approximation theory, a fundamental question is whether polynomials can approximate any given continuous function to an arbitrary degree of precision. Weierstrass [22] provides a definitive answer by:

**Theorem 2.2** (Weierstrass Approximation Theorem) Let  $f(x) \in L^p[0,1]$  for any p > 0. Then there exists an algebraic polynomial  $p_n(x) = \sum_{m=0}^n c_m x^m$  such that

$$\lim_{n \to \infty} \int_0^1 |f(x) - p_n(x)|^p dx = 0.$$
 (3)

This interval can be extended to [a, b]. This demonstrates that polynomials  $p_n \in \mathcal{P}_n$  can serve as basis functions  $\psi(x)$  in Equation (2) to approximate the f in Theorem 2.1. In our task, the vehicle trajectories are treated as the function f, with respect to the time step t. For different driving styles, we employ corresponding  $p_n$  as basis functions to approximate these trajectories in accordance with Theorem 2.2. Furthermore, these trajectories also belong to the  $L^p$  space<sup>2</sup>, and are thus well-defined.

#### 3 Methodology

#### 3.1 Motivation and Overview

Our **D**riving-**S**tyle-**A**daptive (DSA) framework (illustrate in 2) models the behavior of the trajectory originator: the human driver. The **driving style** of various vehicle drivers are categoried as: **C**onservative, **A**ggressive and **N**ormal (CAN) [48, 49, 50], each reflecting distinct trajectory characteristics.

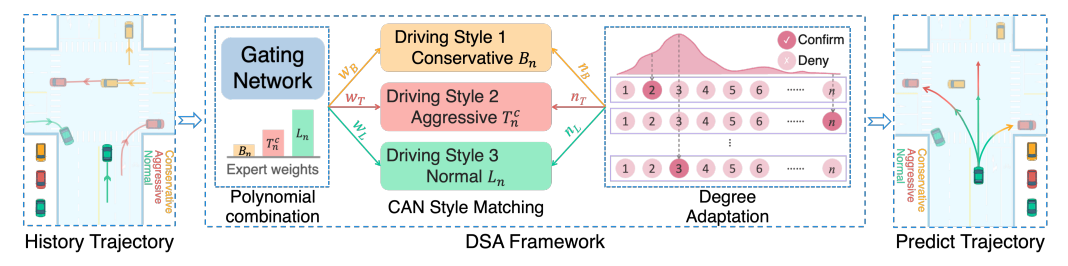


Figure 2: An overview of our DSA framework, which performs trajectory prediction based on driving style categories: conservative, aggressive and normal (CAN) to prediction. For clarity, we illustrate this process using a single vehicle example. the solid line represents trajectories length while the arrow ndicates the direction (history or future). The symbol  $B_n$ ,  $T_n^c$  and  $L_n$  denote different basis functions  $p_n$  corresponding to each driving style. Our proposed DSA framework dynamic adaps the experts (driving style) weighs  $w_*$  and the degree  $n_*$  of selected  $p_n$ .

We match each driving style characteristic to a corresponding approximation polynomial  $p_n$  based on the mathematics properties of  $p_n$  as described in Section 3.2. To implement this mechanism, we introduce  $p_n$  combination and degree adjustment strategies in Section 3.3.

<sup>&</sup>lt;sup>2</sup>Taking the x-position as an example, it can be shown that the integral  $\int_{\Omega} |x(t)| dt < \infty$  holds

#### 3.2 Theoretical Foundations for Matching Polynomials to Driving Styles

In this section, we elucidate the matching between the polynomials  $p_n$  ( $p_n \in \mathcal{P}_n$ ) and driving style, focusing on the mathematical properties of  $p_n$  and analyzing the characteristics of each driver's type. Specifically, we address conservative drivers in Section 3.2.1, aggressive drivers in Section 3.2.2 and normal drivers in Section 3.2.3.

#### 3.2.1 Conservative Drivers

Conservative drivers [51] prioritize driving comfort and safety, which leads to more cautious decisions. Their average speed is typically the slowest and rarely change their behavior. Consequently, their trajectories are characterized by smoothness and stability, with minimal abrupt changes in speed.

In this situation, we require a  $p_n$  to capture approximating drivers with minimal behavioral changes, that is, ensures the approximation error decreases uniformly across the entire interval. we employ the Bernstein operatore<sup>3</sup>  $B_n$  [52] to achieve this:

**Definition 3.1** (Bernstein polynomial,  $B_n$ ) Consider a function  $f(x) \in C[0,1], x \in [0,1], B_n$  is specified by the equation:

$$(B_n) f(x) = \sum_{k=0}^n f\left(\frac{k}{n}\right) \binom{n}{k} x^k (1-x)^{n-k}.$$

 $\left(B_n\right)f\left(x\right)=\sum_{k=0}^n f\left(\frac{k}{n}\right)\binom{n}{k}\,x^k\,(1-x)^{n-k}\,.$  It is clear that  $B_n\subseteq\mathcal{P}_n$  thus applies to Theorem 2.2. The primary advantage of the  $B_n$  is articulated in the following proposition:

**Proposition 3.2** For all functions  $f \in C[0,1]$ , the sequence  $\{B_n f; n=1,2,3,\cdots\}$  converges uniform<sup>4</sup> to f as  $B_n(f) \rightrightarrows f(x)$ .

This proposition demonstrates that the  $B_n$  exhibits uniform convergence across the entire interval, making it particularly suitable for approximating trajectories with slow travel speeds and few behavioral changes, such as those of conservative drivers. This ensures that the approximation error decreases uniformly throughout the interval.

#### 3.2.2 Aggressive Drivers

Aggressive drivers [53] prioritize their own benefits at the expense of safety and comfort, which leads to higher speeds, abrupt changes in acceleration and braking, with a frequent tendency to change lanes. As a result, their trajectories display more abrupt motions and are less smooth.

Trigonometric polynomials  $T_n$  are dense<sup>5</sup> in C(I) on the unit circle according to the Stone-Weierstrass Theorem [54]. This implies that trigonometric polynomials  $T_n$  are particularly effective at approximating functions with discontinuities or sharp features, which define as:  $T_n(x) = a_0 + \sum_{n=1}^{N} \left[ a_n \cos(nx) + b_n \sin(nx) \right]$ . We employ the Chebyshev polynomials [55]  $T_n^c$ , defined as follows:

**Definition 3.3** (Chebyshev Polynomials,  $T_n^c$ ) For  $x \in [-1, 1]$ , the n-th  $T_n^c$  of the first kind is given by  $T_n^c(x) = \cos[n \cdot \arccos(x)].$ 

The effectiveness of  $T_n^c$  is further highlighted by the Chebyshev Minimax Theorem [56]:

**Theorem 3.4** (Chebyshev Minimax Theorem) For  $f \in C[-1,1]$ ,  $T_n^c$  minimizes the maximum error in the uniform norm compared to any other  $p_n$  approximation of the same degree. Formally, this relationship is expressed as:

$$||f - T_n^c||_{L^{\infty}} \leqslant ||f - p_n||_{L^{\infty}}.$$

<sup>&</sup>lt;sup>3</sup>In this task, we leverage  $p_n$  approximation operators to approximate and predict the vehicle trajectories, Specifically, we instantiate these operators using representative basis such as  $B_n$ , the same as other two approximation operators.

<sup>&</sup>lt;sup>4</sup>Uniform Convergence For every  $\epsilon > 0$ , there exists an  $N \in \mathbb{Z}^+$ ,  $N = N(\epsilon)$ , s.t. for all  $n \ge N$ , there is  $|f_n(x) - f(x)| < \epsilon.$ 

<sup>&</sup>lt;sup>5</sup>**Dense** A subset A of a topological space X is said to be dense in X if every point of X either belongs to A or else is arbitrarily "close" to a member of A.

Theorem 3.4 explicitly states that  $T_n^c$  can minimize the maximum error, effectively reducing the impact of sudden behavioral and speed changes typical of aggressive drivers. Furthermore, the overall prediction error is decreased.

#### 3.2.3 Normal Drivers

Normal drivers [57] strike a balance between conservative and aggressive driving styles, representing a relatively common group in driving behavior. Their speed and acceleration typically fall between those of conservative and aggressive drivers, exhibiting moderate speed changes and occasional rapid reactions. Consequently, their trajectories are neither as smooth as those of conservative drivers nor as abrupt as those of aggressive drivers, but their trajectories may exhibit regular fluctuations.

This driving characteristic is closely related to the application of orthogonal polynomials  $p_n^o$  [58]. The  $p_n^o$  has significant flexibility and enables accurately capture the trajectories characterized by gradual changes and moderate fluctuations for normal drivers. The  $p_n^o$  with weight function  $\rho$  and  $\partial (p_n^o) = n$  are defined as:  $\langle p_i^o, p_j^o \rangle = \int_a^b \rho(x) \, p_i^o(x) \, p_j^o(x) \, dx = \delta_{ij}$ , where  $\delta_{ij}$  equal to 0 iff  $i \neq j$ . The approximation of  $p_n^o$  can be effectively described by [59]:

**Theorem 3.5** (Least Squares Characterization Theorem) For any function  $f \in C[a,b]$ , there exists an orthogonal polynomial  $p_n^o$  with  $\partial (p_n^o) \leq n$  that minimizes the error in the  $L_\rho^2$  norm<sup>7</sup> between f(x) and  $p_n^o(x)$ :

$$||f - p_n^o||_{L^2_\rho} = \min_{p \in \mathbb{P}_n} ||f - p||_{L^2_\rho},$$

where  $P_n$  denotes the space of all polynomials of degree at most n.

The term "least" here does not denote the non-uniqueness, but rather indicates the possible to select optimal coefficients under best  $L_{\rho}^2$  approximating. For instance, Legendre polynomials  $L_n$  is a typical orthogonal polynomial:

**Definition 3.6** (Legendre Polynomial,  $L_n$ ) For  $x \in [-1, 1]$  with a constant weight function  $\rho(x) = 1$ ,  $L_n$  is defined by

$$L_n = \frac{1}{2^n n!} \frac{d^n}{dx^n} \left[ \left( x^2 - 1 \right)^n \right].$$

This orthogonality under the  $L^2$  norm particularly without weight or a constant weight, makes it an exceptionally efficient tool for approximation [60], which represents a specific instance covered by Theorem 3.5. Moreover,  $L_n$  is also defined by a simple recurrence relation:

$$(n+1)L_{n+1}(x) = (2n+1)xL_n(x) - nL_{n-1}(x),$$

This recurrence relation facilitates quick calculations and the optimal square approximation property excels under the  $L^2$  norm. These characteristics make it well-suited for handling smooth and continuous trajectory fluctuations, align well with the The normal drivers. Their characterized by gradual changes and smoother transitions.

#### 3.3 Algorithm Realization

#### 3.3.1 Polynomial Combination

In Section 3.2, we utilize different polynomial forms to match different driving styles, thereby fully leveraging trajectory information for prediction. However, assuming a single fixed driving style may be inadequate in complex real-world scenarios. Kernel density estimation and latent variable analysis, reveal that driver behavior varies continuously with context and can be characterized as a probabilistic mixture [21, 61, 62] of weighted driving styles. Here we employ a MoE-TopK [63] approach to model multiple driving styles for trajectory prediction.

<sup>&</sup>lt;sup>6</sup>Weight Function In open interval (a, b), the defined positive, continuous, and integrable function is called weight function.

The  $L^2_{\rho}$  Norm Used to measure the "magnitude" or "error" of a function when combined with a particular weighting function  $\rho(x)$  in a given interval. It is defined as  $\|f\|_{L^2_{\rho}} = \left(\int_a^b |f(x)|^2 \rho(x)\,dx\right)^{1/2}$ .

The process of combining the polynomials corresponding to multiple driving styles is presented in the algorithm on the right. Here  $X_i$  represents the i-th history trajectory in N vehicles as described in Section 2.1, which has 5 dimensions as (x,y) position, velocity, acceleration, and the nearest lane segments ID. Experts represents the polynomials in Section 3.2. The output  $z^{\text{Com}}$  is the feature of combine. In line 2, "SN" and "Sp" denote the Standard Normal and Softplus functions [64, 65], respectively,  $W_q$  and  $W_n$  are trainable weight matrices. In line 3, we define  $H = (H_1, H_2, H_3)$ .

This combination structure of  $p_n$  allows each  $E_i$  to better extract the trajectory feature in different driving styles, and enables the use of various basis functions for predict vehicle trajectory. To encourage all experts to contribute the combination process, Shazeer N et al. [63] introduce a load balancing loss function  $L_{\text{MoE-K}}$  to encourage experts have equal importance as:  $L_{\text{MoE-K}} = w_{\text{load}} \cdot \text{CV} (\text{loads})^2$ , where "CV" denotes the coefficient of variation.

#### **Algorithm: Polynomial Combination**

**Require:** Input vehicle trajectory  $X_i$ , 1: Experts networ  $\{E_j\}_{j=1}^3$ , Gating network G **Ensure:** Feature  $z_i^{\operatorname{Com}}$  via Polynomial Combination 2:  $H_j \leftarrow (X \cdot W_g)_i + \operatorname{SN}() \cdot \operatorname{Sp}[(X \cdot W_n)_i]$  for all i 3:  $G_j(x) = \operatorname{Softmax}(H)$  4: **for** i = 1 to N **do** 5:  $z_i^{\operatorname{Com}} \leftarrow G_j(X_i) \cdot E_j(X_i)$ . 6: **end for** 7:  $z_i^{\operatorname{Com}} \leftarrow \sum_{i=1}^N z_i^{\operatorname{Com}}$ 

#### 3.3.2 Degree Adjustment

Different driving style of trajectories can be approximated by corresponding  $p_n$ . However, the fixed degree of  $p_n$  can restrict their ability for prediction entire trajectory of vehicles, which refers to:

**Theorem 3.7** (Kolmogorov Theorem) For  $f \in C[a,b]$ , there exists a polynomial  $p_n$  such that approximation error is bounded by:

$$||f - P_n||_{L^{\infty}} \lesssim \left(\frac{\log n}{n}\right) V(f, [a, b]),$$

where V(f, [a, b]) denotes the total variation<sup>8</sup> of f over the interval.

From Theorem 3.7, the accuracy of the polynomial approximation is directly related to the degree n of the  $p_n$ , which applies broadly to  $L^p$ -space. On the other hand, the n is bounded when error bounded of  $p_n$  is know, this assertion is proved in Appendix  $\mathbb{C}$ .

Adapting n presents a complex non-convex and combinatorial optimization problem. To tackle this issue, we utilize SMAC3 [66] tool, which is particularly suitable for optimizing low-dimensional and continuous functions, suitable for characteristic of vehicle trajectory (Section 2.1). Specifically, the degree n is treated as a hyperparameter optimization problem, aimed at minimizing the loss (L) on validation data  $D_{\rm val}$  and training data  $D_{\rm train}$ . This process can be formulated as follows:

$$n_{\text{SMAC}} \in \underset{n \in \mathbb{Z}^+}{\arg\min} \ c\left(n\right) = \underset{n \in \mathbb{Z}^+}{\arg\min} \ L\left(\mathcal{D}_{\text{train}}, \mathcal{D}_{\text{val}}; n\right),$$

The hyperparameter optimization process targets the final degree  $n_{\rm SMAC}$ , corresponding to achieve the least error for the corresponding basis function  $p_n$ .

#### 4 Experiments

#### 4.1 Basic Setting

We evaluate our DSA framework on three real-world vehicle trajectory prediction datasets: nuScenes [67], Argoverse [68] and Waymo [69]. These timestep settings follow the format(history time  $\rightarrow$  prediction time):  $2 \rightarrow 6$ ,  $2 \rightarrow 3$  and  $1 \rightarrow 8$ , respectively. We utilize  $L_{\rm oss} = \lambda_1 L_{\rm Dis} + \lambda_2 L_{\rm MoE-K}$ , with  $L_{\rm MoE-K} = w_{\rm load} \cdot {\rm CV} \left({\rm loads}\right)^2$  for model training with balanced weighting parameters  $\lambda_*$ . We employ common standard metrics as the Average / Final Displacement Error (ADE / FDE) for evaluate generate k trajectories. More detail of datasets and metrics, please refer to Appendix B.

<sup>&</sup>lt;sup>8</sup>**Total Variation** A measure of the total amount of variation in a function over a given interval [a,b], which is defined by  $\sup_{x\neq y}|f(x)-f(y)|/|x-y|$ .

#### 4.2 Main Results

#### 4.2.1 Quantitative Result

We evaluate our proposed DSA framework against existing methods utilize standard metrics. The **best** and **second-best** results are highlighted in Table 1 for the nuScenes and Argoverse datasets (with a 2-second observation window). Table 2 for Waymo (with a 1-second observation window) respectively. The results demonstrate that our method outperforms most existing approaches, achieving superior performance in 9 out of 13 evaluation metrics and ranking second in 3 others. Specifically, the best results over baseline datasets in Section 4.1 are 5.52%-FDE<sub>5</sub> (nuScenes), 8.82% -ADE<sub>6</sub> (Argoverse) and 1.93%-minFDE (Waymo).

Table 1: Performance comparison of baseline and our DSA framework on the nuScenes (left, N-Method) and Argoverse (right, A-Method) datasets. The **best** and **second-best** are highlighted.

N-Method	$ADE_1$	$FDE_1$	$ADE_5$	$FDE_5$	$ADE_{10}$	FDE <sub>10</sub>	A-Method	$ADE_1$	$FDE_1$	$ADE_6$	FDE <sub>6</sub>
THOMAS [70]	-	6.71	1.33	-	1.04	-	GOHOME [71]	1.70	3.68	0.89	1.29
PreTraM [72]	-	-	1.70	4.15	1.45	3.22	LTP [13]	1.62	3.55	0.83	1.30
Goal-Driven [73]	-	-	1.85	3.87	1.32	2.50	MP++* [74]	1.62	3.61	0.79	1.21
MUSE-VAE [75]	-	-	1.38	2.90	1.09	2.10	HiVT [76]	1.60	3.53	0.77	1.17
Real-Time [77]	3.56	8.63	1.60	3.34	1.23	2.32	ADAPT [78]	1.59	3.50	0.79	1.17
Aware [79]	5.58	11.47	-	-	1.67	2.66	Aware [79]	1.61	3.54	0.86	1.31
FRM [80]	-	6.59	1.18	-	0.88	-	FRM [80]	-	-	0.82	1.27
Context-Aware [81]	3.54	8.24	1.59	3.28	-	-	R-Pred [82]	1.58	3.47	0.76	1.12
LAformer [11]	-	-	1.19	-	0.93	-	LAformer [11]	-	-	0.77	1.16
DAMM [83]	2.84	6.59	1.39	3.14	1.02	2.05	DAMM [83]	1.57	3.42	0.76	1.29
CASPNet++ [84]	2.74	6.18	1.16	-	0.92	-	ProphNet [85]	1.28	2.77	0.68	0.97
CASPFormer [86]	-	6.70	1.15	-	-	-	QCNet [87]	-	-	0.73	1.07
DSA	2.69	6.47	1.21	2.74	0.85	2.00	DSA	1.17	2.85	0.62	0.95

In the nuScenes dataset, DSA outperforms previous methods in metrics of ADE $_1$ , FDE $_5$ , ADE $_{10}$ , and FDE $_{10}$ . Compared to DAMM [83], which utilizes higher-order patterns to describe interactions between agents (vehicles), our model shows a significant improvement, achieving a 16.67% enhancement in ADE $_{10}$ . Moreover, compared with FRM [80], which uses lane information to predict stochastic future relationships among agents, there is only a marginal gap of 0.03 in ADE $_5$ , but we achieve a 3.41% improvement in ADE $_{10}$ . However, DSA is slightly less effective than CASPNet++[84], which employs interaction modeling and scene understanding for joint prediction of all road users while we only predict vehicle, that leads to a minimal gap, measured in the thousandth place.

In the Argoverse dataset, our model achieves on three of four metrics in baseline. Although our FDE<sub>1</sub> metric gap in 0.08 than the baseline best results ProphNet [85], when predicting 6 samples, DSA shows improvements of 8.82% in ADE and 2.06% in ADE. In addition, while ProphNet utilizes an agent-centric model with anchor informed strategies, our DSA employs global positioning directly.

In the Waymo dataset (Table 2), our DSA achieve the lowest minFDE and MR. We reduce the MR by 5.14% and minFDE by 1.88% compared to MotionLM [94], their minADE is slightly higher than ours by 0.015, whereas our framework is based on a simpler baseline model The ControlMTR [97] generate scene-compliant intention points and converte into a physics-based model, while DSA is driving and mathematical based, we reduce the minFDE with 4.10% (value 0.0488).

Table 2: Performance comparison of baseline and our DSA framework on the Waymo datasets. The **best** and **second-best** are highlighted.

Method	minADE	minFDE	MR*
MultiPath++ [74]	0.9780	2.3050	0.4400
SceneTransformer [88]	0.6117	1.2116	0.1564
MPA [89]	0.5913	1.2507	0.1603
ReCoAt [90]	0.7703	1.6668	0.2437
DIPP [91]	0.6951	1.4678	0.1854
LiMTR [92]	1.3640	-	0.2156
HDGT [93]	0.5933	1.2055	0.1511
MotionLM [94]	0.5702	1.1653	0.1327
MTR++ [95]	0.5912	1.1986	0.1296
TC-Map [96]	0.6181	1.2375	0.1402
ControlMTR [97]	0.5897	1.1916	0.1262
DSA	0.5852	1.1431	0.1259

<sup>\*</sup> MR (Missing Rate) is the proportion of cases in which the Euclidean distance between the prediction and the ground truth at FDE exceeds 2m.

Our DSA framework adaptive design accommo-

dates three categories of driving styles and we provide comprehensive explanations. This strategy simplifies the prediction process and enhances the accuracy and adaptability of predictions in complex real-world traffic scenarios.

#### 4.2.2 Qualitative Result

Figure 3 demonstrates the effectiveness for our DSA framework in vehicle trajectories prediction. For more visual content, please refer to Appendix. The k is the number of generation trajectories, ground truth trajectory is actual trajectories. To describe specific subfigures in Figure 3, we use the

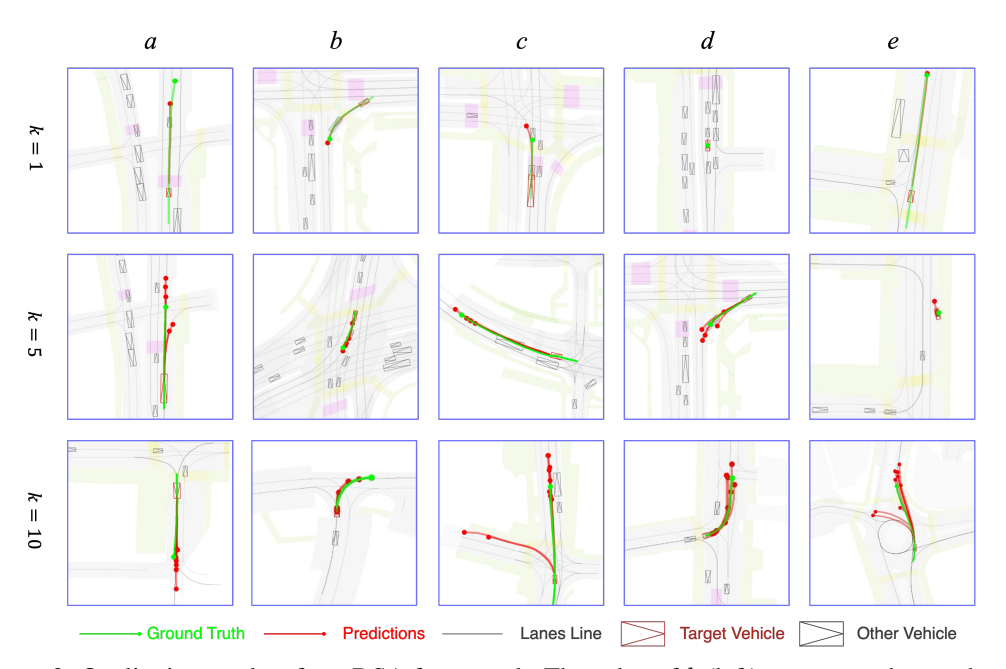


Figure 3: Qualitative results of our DSA framework. The value of k (left) represents the number of generation trajectories while letters (top) are index for clearly describe. Round head lines represents predict and ground truth trajectory, respectively.

position index (k, \*) where \* denotes the letter shown at the top of each subfigure.

When k=1 (i.e. the first row of Figure 3), he single prediction samples demonstrate that our DSA framework generally produces accurate results. It effectively handles not only simple road scenarios: such as straight lanes in (1,a) and (1,e), or stop conditions in (1,d). But also complex scenarios including T-junctions in (1,b) and crossroads in (1,c).

In cases for generates 5 and 10 trajectories, our DSA framework delivers predictions that are both accurate and diverse. In simple scenarios, such as go straight in (5,c), (10,a), or stopping in (5,e), our framework maintains high accuracy while offering a broader range of plausible outcomes. It particularly excels in complex road conditions, including Y-crossroads in (10,b), high density crossroads (5,b) and roundabouts (10,e). Moreover, the predicted trajectories effectively conform to curved roads, such as turning maneuvers in (5,d) and (10,d).

#### 4.3 Ablation Studies for DSA Framework

To explore the benefits of different components and design choices in our DSA framework, we conduct ablation experiments along several dimensions: Type and combination of polynomials  $p_n$  in Section 4.3.1. Degree adjustment of polynomials in Section 4.3.2. Analysis of driving style in Section 4.3.3, examining the relationship between styles and specific  $p_n$ , and how expert weights reflect behaviors. In addition, we present sensitivity analyses for different scenarios in Appendix D.

#### 4.3.1 Effects of Approximate Polynomial

We design two experiments to evaluate the combination and type of  $p_n$  on the Argoverse dataset. **The number of polynomials.** To illustrate the importance of considering all drivers' driving styles instead of the parts of them in trajectory predictions, we simulate a scenario where only one or two driving styles existing and select corresponding matching  $p_n$  (Section 3.2) for prediction.

Analyzing results from Table 3, consider whole driving style outperform almost the best than other combine. We observe that DSA framework incorporating two driving styles generally outperform those with only one. However, this trend is not universal. For instance, in FDE<sub>1</sub>, the model

based solely on the normal driver (1.32) over the combination of conservative and aggressive styles (C+A, 1.54). Compared to the above combine (C+A) in ADE<sub>6</sub>, DSA further re-

Table 3: The performances of DSA framework with different combinations of basis functions on the Argoverse dataset. C, A and N denote Conservative- $B_n$ , Aggressive- $T_n^c$  and Normal- $L_n$ , respectively. The **best** and <u>second-best</u> results are highlighted in table.

Metric	С	A	N	C+A	A+N	C+N	DSA
$ADE_1$	1.61	1.45	1.32	1.54	1.39	1.66	1.17
$FDE_1$	3.46	2.87	2.91	3.09	2.87	2.78	2.85
FDE <sub>1</sub> ADE <sub>6</sub>	1.02	1.31	1.12	0.83	0.92	0.98	0.62
$FDE_6$	1.26	1.29	1.33	1.29	1.04	1.17	0.96

duces 0.21 with 25.3%. This illustrate that the necessity of considering all driving styles in trajectory prediction.

Table 4: Evaluate different  $p_n$  in DSA framework on the Argoverse dataset, with original  $\rightarrow$  replace and corresponding style (abbreviate with the first three letters) in the second column. The **best** and second-best results highlight in table.

Method	Replace	$ADE_1$	$FDE_1$	$ADE_6$	$FDE_6$
$C_n + T_n + L_n$	$B_n \to C_n$ Con	1.48	3.76	1.10	1.53
$B_n + S_n + L_n$	$T_n \to S_n \operatorname{Agg}$	1.59	3.91	0.86	1.41
$B_n + T_n + H_n$	$L_n \to H_n$ Nor	1.62	2.81	0.71	1.02
DSA	-	1.17	2.85	0.62	0.96

The Type of Polynomials. For instruction the effects of the  $p_n$  we utilize in DSA framework, we replace types of  $p_n$  to evaluate it, with results in Table 4. We select Charlier ([98],  $C_n$ ), Hermite ([99],  $H_n$ ) and second-order  $(S_n)$  polynomials to instead  $p_n$  we select in our DSA framework.

Our DSA yields the best performance on three out of four evaluation metrics in **blod**, which most improved is 27.8%, 43.6% and 37.3% respectively.

Although the combination  $B_n + T_n + H_n$  achieves a slightly lower FDE<sub>1</sub> from 2.81 to 2.85 by 1.4% a marginal gap, DSA still ranks second on FDE<sub>1</sub>.

#### 4.3.2 Effects of Polynomial Degree

From Theorem 3.7, we understand that the prediction accuracy is directly related to the degree n of the polynomial  $p_n$ . We now evaluate the impact of adaptively adjusting n. To clearly illustrate this influence, we analyze the performance of a single driving style with varying degrees, as shown in Figure 4. We observe that the error generally decreases with an increasing degree. However, the

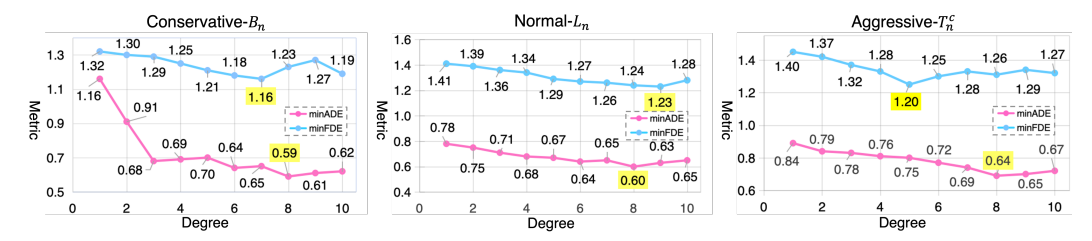


Figure 4: Performance of our DSA Framework, with only one single fixed basis function on the waymo dataset, which the lowest error highlighted in yellow.

highest degree does not necessarily yield the best results. For instance, within the aggressive driver style,  $\partial\left(T_{n}^{c}\right)=5$  outperforms other degrees in minFDE while  $\partial\left(T_{n}^{c}\right)=8$  is the best minADE, similar to conservative and normal driving style, the best results from different degrees. Consequently, adjusting n rather than maintaining a fixed set provides enhanced granularity for the  $p_{n}$  polynomials, thereby improving their capability to generate accurate and varied predictions across diverse vehicle trajectory styles.

#### 4.3.3 Analysis of Driving Style

In Section 3.2, we provide the mathematical analysis for matching driving styles to their corresponding  $p_n$ . Here, we present experimental results that evaluate both the matching relationships and how expert weights reflect those relationships.

# Relationship between driving style and polynomials. We compute the cosine similarity between the trajectory corresponding to the highest-weighted polynomial $p_n$ and the predefined driving style standards [48, 49, 50], which include Conservative (Con), Aggressive (Agg), and Normal (Nor). The results on the nuScenes (from N-Con) and Argoverse (from A-Con) datasets are shown in Table 5

Table 5: Cosine similarity reflecting consistent matching between polynomial based predictions and driving style standards on the nuScenes (N) and Argoverse (A) datasets.

$\overline{p_n}$	N-Con	Agg	Nor	A-Con	Agg	Nor
$B_n$	0.953	0.158	0.489	0.884	0.129	0.391
$T_n$	0.266	0.987	0.353	0.167	0.927	0.329
$L_n$	0.310	0.263	0.992	<b>0.884</b> 0.167 0.206	0.333	0.963

From Table 5, our matching scheme ( $B_n$ -

Con,  $T_n$ -Agg,  $L_n$ -Nor) obtains significantly higher similarity scores on both datasets. On the nuScenes dataset, the average similarity of the three correct matches (diagram values) is 0.977, while that of all other matches (non-bold entries) is 0.307. On Argoverse, these values are 0.925 and 0.259, respectively, representing a substantial gap.

Table 6: The matching relationship between different driving styles and their corresponding  $p_n$ . The percentage indicates the rate at which each  $p_n$  has the highest weight within each driving style.

Style	Argoverse	nuScenes	Top-1
Con	86.15%	87.96%	$B_n$
Agg	92.87%	94.26%	$T_n$
Nor	80.04%	83.56%	$L_n$

Expert weights mapping to driving style. To examine how expert weights mapping to driving styles, we compute the correct matching rate, defined as the proportion of cases in which the highest expert weight (Top-1) matches the expected  $p_n$  for each driving style. The results appear in Table 6. The average correct matching rates across the two datasets are 86.35% and 88.59%, respectively. The highest matching rate is 94.26% for aggressive drivers on the nuScenes dataset. All styles achieve a matching rate above 80%, with a fluctuation range of 14.22%.

#### 5 Limitation

We evaluate our method on prediction horizons up to 9 seconds (1 second of history and 8 seconds of future), which is the longest duration available in current open-access vehicle trajectory datasets. However, for significantly longer horizons (e.g., over one minute), direct long-term prediction may be unreliable and would likely require segment-wise modeling or hierarchical strategies. In addition, external factors such as strong conditions (e.g., traffic signals and regulatory constraints) and soft conditions (e.g., weather, which is often unlabeled in current datasets) can also affect trajectory prediction. Incorporating these contextual cues remains an important direction for future work.

#### 6 Conclusion

We propose an adaptive framework for vehicle trajectory prediction that is tailored to the driving styles of human drivers. To enable effective matching between polynomials  $p_n$  and driving styles, we analyze the behavioral characteristics of each style alongside the mathematical properties of corresponding  $p_n$ . Furthermore, we investigate the effects of  $p_n$  combine, the influence of different polynomial types, and the necessity of adaptive parameters such as degree. Experiments results on three real-world datasets demonstrate that our framework significantly outperforms existing methods.

#### Acknowledgements

This research is sponsored by the National Natural Science Foundation of China (U21B2090, 62472238, 62576181), the National Key Research and Development Program of China (2023YFB4301900), the Shenzhen Science and Technology Program (JCYJ20240813151445059), and the Science and Technology Planning Project of Guangdong Province (2023B12120600291).

#### References

- [1] Penghao Wu, Xiaosong Jia, Li Chen, Junchi Yan, Hongyang Li, and Yu Qiao. Trajectory-guided control prediction for end-to-end autonomous driving: A simple yet strong baseline. *Advances in Neural Information Processing Systems*, 35:6119–6132, 2022.
- [2] Qingzhao Zhang, Shengtuo Hu, Jiachen Sun, Qi Alfred Chen, and Z Morley Mao. On adversarial robustness of trajectory prediction for autonomous vehicles. In *Proceedings of the IEEE/CVF Conference* on Computer Vision and Pattern Recognition, pages 15159–15168, 2022.
- [3] Zhigang Wu, Jiyu Wang, Huanting Xu, and Zhaocheng He. T3c: A traffic-communication coupling control approach for autonomous intersection management system. *Transportation Research Part C: Emerging Technologies*, 169:104886, 2024.
- [4] Haoran Song, Di Luan, Wenchao Ding, Michael Y Wang, and Qifeng Chen. Learning to predict vehicle trajectories with model-based planning. In *Conference on Robot Learning*, pages 1035–1045. PMLR, 2022.
- [5] Hong Wang, Bing Lu, Jun Li, Teng Liu, Yang Xing, Chen Lv, Dongpu Cao, Jingxuan Li, Jinwei Zhang, and Ehsan Hashemi. Risk assessment and mitigation in local path planning for autonomous vehicles with lstm based predictive model. *IEEE Transactions on Automation Science and Engineering*, 19(4):2738–2749, 2021.
- [6] Chalavadi Vishnu, Vineel Abhinav, Debaditya Roy, C Krishna Mohan, and Ch Sobhan Babu. Improving multi-agent trajectory prediction using traffic states on interactive driving scenarios. *IEEE Robotics and Automation Letters*, 8(5):2708–2715, 2023.
- [7] Xiao Han, Xinfeng Zhang, Yiling Wu, Zhenduo Zhang, Tianyu Zhang, and Yaowei Wang. Knowledge-based multiple relations modeling for traffic forecasting. *IEEE Transactions on Intelligent Transportation Systems*, 2024.
- [8] Ye Yuan, Xinshuo Weng, Yanglan Ou, and Kris M Kitani. Agentformer: Agent-aware transformers for socio-temporal multi-agent forecasting. In *Proceedings of the IEEE/CVF International Conference on Computer Vision*, pages 9813–9823, 2021.
- [9] Tung Phan-Minh, Elena Corina Grigore, Freddy A Boulton, Oscar Beijbom, and Eric M Wolff. Covernet: Multimodal behavior prediction using trajectory sets. In *Proceedings of the IEEE/CVF conference on computer vision and pattern recognition*, pages 14074–14083, 2020.
- [10] Jiachen Li, Hengbo Ma, Zhihao Zhang, Jinning Li, and Masayoshi Tomizuka. Spatio-temporal graph dualattention network for multi-agent prediction and tracking. *IEEE Transactions on Intelligent Transportation* Systems, 23(8):10556–10569, 2021.
- [11] Mengmeng Liu, Hao Cheng, Lin Chen, Hellward Broszio, Jiangtao Li, Runjiang Zhao, Monika Sester, and Michael Ying Yang. Laformer: Trajectory prediction for autonomous driving with lane-aware scene constraints. In *Proceedings of the IEEE/CVF Conference on Computer Vision and Pattern Recognition*, pages 2039–2049, 2024.
- [12] Nachiket Deo, Eric Wolff, and Oscar Beijbom. Multimodal trajectory prediction conditioned on lane-graph traversals. In *Conference on Robot Learning*, pages 203–212. PMLR, 2022.
- [13] Jingke Wang, Tengju Ye, Ziqing Gu, and Junbo Chen. Ltp: Lane-based trajectory prediction for autonomous driving. In Proceedings of the IEEE/CVF Conference on Computer Vision and Pattern Recognition, pages 17134–17142, 2022.
- [14] Qingwen Xue, Yingying Xing, and Jian Lu. An integrated lane change prediction model incorporating traffic context based on trajectory data. *Transportation research part C: emerging technologies*, 141:103738, 2022.

- [15] Ross Greer, Nachiket Deo, and Mohan Trivedi. Trajectory prediction in autonomous driving with a lane heading auxiliary loss. *IEEE Robotics and Automation Letters*, 6(3):4907–4914, 2021.
- [16] Haoran Li, Chaozhong Wu, Duanfeng Chu, Liping Lu, and Ken Cheng. Combined trajectory planning and tracking for autonomous vehicle considering driving styles. *IEEE Access*, 9:9453–9463, 2021.
- [17] Maria Valentina Niño de Zepeda, Fanlin Meng, Jinya Su, Xiao-Jun Zeng, and Qian Wang. Dynamic clustering analysis for driving styles identification. *Engineering applications of artificial intelligence*, 97:104096, 2021.
- [18] Harpreet Singh and Ankit Kathuria. Profiling drivers to assess safe and eco-driving behavior—a systematic review of naturalistic driving studies. Accident Analysis & Prevention, 161:106349, 2021.
- [19] Wenshuo Wang, Junqiang Xi, and Ding Zhao. Driving style analysis using primitive driving patterns with bayesian nonparametric approaches. *IEEE Transactions on Intelligent Transportation Systems*, 20(8):2986–2998, 2018.
- [20] Ziming Liu, Yixuan Wang, Sachin Vaidya, Fabian Ruehle, James Halverson, Marin Soljačić, Thomas Y Hou, and Max Tegmark. Kan: Kolmogorov-arnold networks. arXiv preprint arXiv:2404.19756, 2024.
- [21] Wei Han, Wenshuo Wang, Xiaohan Li, and Junqiang Xi. Statistical-based approach for driving style recognition using bayesian probability with kernel density estimation. *IET Intelligent Transport Systems*, 13(1):22–30, 2019.
- [22] K WEIERSTRASS. Über die analytische darstellbarkeit sogenannter willkürlicher funktionen einer reellen. 1885.
- [23] Zhezhang Ding and Huijing Zhao. Incorporating driving knowledge in deep learning based vehicle trajectory prediction: A survey. IEEE Transactions on Intelligent Vehicles, 8(8):3996–4015, 2023.
- [24] Jingke Wang, Tengju Ye, Ziqing Gu, and Junbo Chen. Ltp: Lane-based trajectory prediction for autonomous driving. In Proceedings of the IEEE/CVF Conference on Computer Vision and Pattern Recognition, pages 17134–17142, 2022.
- [25] Tim Salzmann, Boris Ivanovic, Punarjay Chakravarty, and Marco Pavone. Trajectron++: Dynamically-feasible trajectory forecasting with heterogeneous data. In Computer Vision–ECCV 2020: 16th European Conference, Glasgow, UK, August 23–28, 2020, Proceedings, Part XVIII 16, pages 683–700. Springer, 2020.
- [26] Xidong Feng, Zhepeng Cen, Jianming Hu, and Yi Zhang. Vehicle trajectory prediction using intention-based conditional variational autoencoder. In 2019 IEEE Intelligent Transportation Systems Conference (ITSC), pages 3514–3519. IEEE, 2019.
- [27] Yutong Ban, Xiao Li, Guy Rosman, Igor Gilitschenski, Ozanan Meireles, Sertac Karaman, and Daniela Rus. A deep concept graph network for interaction-aware trajectory prediction. In 2022 International Conference on Robotics and Automation (ICRA), pages 8992–8998. IEEE, 2022.
- [28] Sumit Kumar, Yiming Gu, Jerrick Hoang, Galen Clark Haynes, and Micol Marchetti-Bowick. Interaction-based trajectory prediction over a hybrid traffic graph. In 2021 IEEE/RSJ International Conference on Intelligent Robots and Systems (IROS), pages 5530–5535. IEEE, 2021.
- [29] Yu Wang, Shengjie Zhao, Rongqing Zhang, Xiang Cheng, and Liuqing Yang. Multi-vehicle collaborative learning for trajectory prediction with spatio-temporal tensor fusion. *IEEE Transactions on Intelligent Transportation Systems*, 23(1):236–248, 2020.
- [30] Kaouther Messaoud, Itheri Yahiaoui, Anne Verroust-Blondet, and Fawzi Nashashibi. Attention based vehicle trajectory prediction. IEEE Transactions on Intelligent Vehicles, 6(1):175–185, 2020.
- [31] Dongwei Xu, Xuetian Shang, Yewanze Liu, Hang Peng, and Haijian Li. Group vehicle trajectory prediction with global spatio-temporal graph. *IEEE Transactions on Intelligent Vehicles*, 8(2):1219–1229, 2022.
- [32] Tao Yang, Zhixiong Nan, He Zhang, Shitao Chen, and Nanning Zheng. Traffic agent trajectory prediction using social convolution and attention mechanism. In 2020 IEEE Intelligent Vehicles Symposium (IV), pages 278–283. IEEE, 2020.
- [33] Andreĭ Nikolaevich Kolmogorov. On the representation of continuous functions of several variables by superpositions of continuous functions of a smaller number of variables. American Mathematical Society, 1961.

- [34] Andrei Nikolaevich Kolmogorov. On the representation of continuous functions of many variables by superposition of continuous functions of one variable and addition. In *Doklady Akademii Nauk*, volume 114, pages 953–956. Russian Academy of Sciences, 1957.
- [35] Jürgen Braun and Michael Griebel. On a constructive proof of kolmogorov's superposition theorem. *Constructive approximation*, 30:653–675, 2009.
- [36] Andrei Nikolaevich Kolmogorov. On the representation of continuous functions of many variables by superposition of continuous functions of one variable and addition. In *Doklady Akademii Nauk*, volume 114, pages 953–956. Russian Academy of Sciences, 1957.
- [37] Vladimir Igorevich Arnol'd. On the representation of continuous functions of three variables by superpositions of continuous functions of two variables. *Matematicheskii Sbornik*, 90(1):3–74, 1959.
- [38] Věra Kůrková. Kolmogorov's theorem is relevant. Neural computation, 3(4):617–622, 1991.
- [39] Martin Riedmiller. Advanced supervised learning in multi-layer perceptrons—from backpropagation to adaptive learning algorithms. *Computer Standards & Interfaces*, 16(3):265–278, 1994.
- [40] Rudolf Kruse, Sanaz Mostaghim, Christian Borgelt, Christian Braune, and Matthias Steinbrecher. Multilayer perceptrons. In Computational intelligence: a methodological introduction, pages 53–124. Springer, 2022.
- [41] Songtao Huang, Zhen Zhao, Can Li, and Lei Bai. Timekan: Kan-based frequency decomposition learning architecture for long-term time series forecasting. *arXiv* preprint arXiv:2502.06910, 2025.
- [42] Diab W Abueidda, Panos Pantidis, and Mostafa E Mobasher. Deepokan: Deep operator network based on kolmogorov arnold networks for mechanics problems. *Computer Methods in Applied Mechanics and Engineering*, 436:117699, 2025.
- [43] Chenxin Li, Xinyu Liu, Wuyang Li, Cheng Wang, Hengyu Liu, Yifan Liu, Zhen Chen, and Yixuan Yuan. U-kan makes strong backbone for medical image segmentation and generation. arXiv preprint arXiv:2406.02918, 2024.
- [44] Benjamin C Koenig, Suyong Kim, and Sili Deng. Kan-odes: Kolmogorov-arnold network ordinary differential equations for learning dynamical systems and hidden physics. *Computer Methods in Applied Mechanics and Engineering*, 432:117397, 2024.
- [45] Alireza Afzal Aghaei. fkan: Fractional kolmogorov-arnold networks with trainable jacobi basis functions. *Neurocomputing*, page 129414, 2025.
- [46] Akash Kundu, Aritra Sarkar, and Abhishek Sadhu. Kanqas: Kolmogorov-arnold network for quantum architecture search. *EPJ Quantum Technology*, 11(1):76, 2024.
- [47] Khemraj Shukla, Juan Diego Toscano, Zhicheng Wang, Zongren Zou, and George Em Karniadakis. A comprehensive and fair comparison between mlp and kan representations for differential equations and operator networks. Computer Methods in Applied Mechanics and Engineering, 431:117290, 2024.
- [48] John Smith and Jane Doe. Real-time driving style classification based on short-term observations. *Transportation Research Part A: Policy and Practice*, 135:105–116, 2021.
- [49] Clara Marina Martinez, Mira Heucke, Fei-Yue Wang, Bo Gao, and Dongpu Cao. Driving style recognition for intelligent vehicle control and advanced driver assistance: A survey. *IEEE Transactions on Intelligent Transportation Systems*, 19(3):666–676, 2017.
- [50] Shiyu Fang, Peng Hang, Chongfeng Wei, Yang Xing, and Jian Sun. Cooperative driving of connected autonomous vehicles in heterogeneous mixed traffic: A game theoretic approach. *IEEE Transactions on Intelligent Vehicles*, 2024.
- [51] Nour O Khanfar, Mohammed Elhenawy, Huthaifa I Ashqar, Qinaat Hussain, and Wael KM Alhajyaseen. Driving behavior classification at signalized intersections using vehicle kinematics: Application of unsupervised machine learning. *International journal of injury control and safety promotion*, 30(1):34–44, 2023.
- [52] S Bernstein. Proof of the theorem of weierstrass based on the calculus of probabilities. *Communications of the Kharkov Mathematical Society*, 13:1–2, 1912.
- [53] Jin-Hyuk Hong, Ben Margines, and Anind K Dey. A smartphone-based sensing platform to model aggressive driving behaviors. In *Proceedings of the sigchi conference on human factors in computing* systems, pages 4047–4056, 2014.

- [54] Walter Rudin et al. Principles of mathematical analysis, volume 3. McGraw-hill New York, 1964.
- [55] Cornelius Lanczos. Solution of systems of linear equations by minimized iterations. J. Res. Nat. Bur. Standards, 49(1):33–53, 1952.
- [56] Theodore J Rivlin. An introduction to the approximation of functions. Courier Corporation, 1981.
- [57] Ahmad Aljaafreh, Nabeel Alshabatat, and Munaf S Najim Al-Din. Driving style recognition using fuzzy logic. In 2012 IEEE International Conference on Vehicular Electronics and Safety (ICVES 2012), pages 460–463. IEEE, 2012.
- [58] Gabor Szeg. Orthogonal polynomials, volume 23. American Mathematical Soc., 1939.
- [59] Theodore S Chihara. An introduction to orthogonal polynomials. Courier Corporation, 2011.
- [60] George E Andrews, Richard Askey, Ranjan Roy, Ranjan Roy, and Richard Askey. Special functions, volume 71. Cambridge university press Cambridge, 1999.
- [61] Chaopeng Zhang, Wenshuo Wang, Zhaokun Chen, Jian Zhang, Lijun Sun, and Junqiang Xi. Shareable driving style learning and analysis with a hierarchical latent model. *IEEE Transactions on Intelligent Transportation Systems*, 2024.
- [62] Dian Jing, Enjian Yao, and Rongsheng Chen. Decentralized human-like control strategy of mixed-flow multi-vehicle interactions at uncontrolled intersections: A game-theoretic approach. *Transportation Research Part C: Emerging Technologies*, 167:104835, 2024.
- [63] Noam Shazeer, Azalia Mirhoseini, Krzysztof Maziarz, Andy Davis, Quoc Le, Geoffrey Hinton, and Jeff Dean. Outrageously large neural networks: The sparsely-gated mixture-of-experts layer. *arXiv preprint arXiv:1701.06538*, 2017.
- [64] Günter Klambauer, Thomas Unterthiner, Andreas Mayr, and Sepp Hochreiter. Self-normalizing neural networks. Advances in neural information processing systems, 30, 2017.
- [65] Hao Zheng, Zhanlei Yang, Wenju Liu, Jizhong Liang, and Yanpeng Li. Improving deep neural networks using softplus units. In 2015 International joint conference on neural networks (IJCNN), pages 1–4. IEEE, 2015.
- [66] Marius Lindauer, Katharina Eggensperger, Matthias Feurer, André Biedenkapp, Difan Deng, Carolin Benjamins, Tim Ruhkopf, René Sass, and Frank Hutter. Smac3: A versatile bayesian optimization package for hyperparameter optimization. *Journal of Machine Learning Research*, 23(54):1–9, 2022.
- [67] Holger Caesar, Varun Bankiti, Alex H. Lang, Sourabh Vora, Venice Erin Liong, Qiang Xu, Anush Krishnan, Yu Pan, Giancarlo Baldan, and Oscar Beijbom. nuscenes: A multimodal dataset for autonomous driving. *arXiv preprint arXiv:1903.11027*, 2019.
- [68] Ming-Fang Chang, John W Lambert, Patsorn Sangkloy, Jagjeet Singh, Slawomir Bak, Andrew Hartnett, De Wang, Peter Carr, Simon Lucey, Deva Ramanan, and James Hays. Argoverse: 3d tracking and forecasting with rich maps. In Conference on Computer Vision and Pattern Recognition (CVPR), 2019.
- [69] Pei Sun, Henrik Kretzschmar, Xerxes Dotiwalla, Aurelien Chouard, Vijaysai Patnaik, Paul Tsui, James Guo, Yin Zhou, Yuning Chai, Benjamin Caine, et al. Scalability in perception for autonomous driving: Waymo open dataset. In *Proceedings of the IEEE/CVF conference on computer vision and pattern recognition*, pages 2446–2454, 2020.
- [70] Thomas Gilles, Stefano Sabatini, Dzmitry Tsishkou, Bogdan Stanciulescu, and Fabien Moutarde. Thomas: Trajectory heatmap output with learned multi-agent sampling. In *International Conference on Learning Representations*, 2022.
- [71] Thomas Gilles, Stefano Sabatini, Dzmitry Tsishkou, Bogdan Stanciulescu, and Fabien Moutarde. Gohome: Graph-oriented heatmap output for future motion estimation. In 2022 international conference on robotics and automation (ICRA), pages 9107–9114. IEEE, 2022.
- [72] Chenfeng Xu, Tian Li, Chen Tang, Lingfeng Sun, Kurt Keutzer, Masayoshi Tomizuka, Alireza Fathi, and Wei Zhan. Pretram: Self-supervised pre-training via connecting trajectory and map. In Computer Vision–ECCV 2022: 17th European Conference, Tel Aviv, Israel, October 23–27, 2022, Proceedings, Part XXXIX, pages 34–50. Springer, 2022.
- [73] Chuhua Wang, Yuchen Wang, Mingze Xu, and David J Crandall. Stepwise goal-driven networks for trajectory prediction. *IEEE Robotics and Automation Letters*, 7(2):2716–2723, 2022.

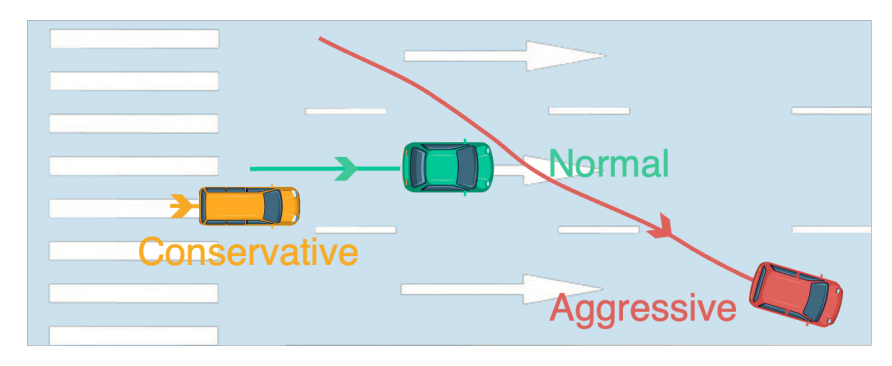
- [74] Balakrishnan Varadarajan, Ahmed Hefny, Avikalp Srivastava, Khaled S Refaat, Nigamaa Nayakanti, Andre Cornman, Kan Chen, Bertrand Douillard, Chi Pang Lam, Dragomir Anguelov, et al. Multipath++: Efficient information fusion and trajectory aggregation for behavior prediction. In 2022 International Conference on Robotics and Automation (ICRA), pages 7814–7821. IEEE, 2022.
- [75] Mihee Lee, Samuel S Sohn, Seonghyeon Moon, Sejong Yoon, Mubbasir Kapadia, and Vladimir Pavlovic. Muse-vae: multi-scale vae for environment-aware long term trajectory prediction. In *Proceedings of the IEEE/CVF Conference on Computer Vision and Pattern Recognition*, pages 2221–2230, 2022.
- [76] Zikang Zhou, Luyao Ye, Jianping Wang, Kui Wu, and Kejie Lu. Hivt: Hierarchical vector transformer for multi-agent motion prediction. In *Proceedings of the IEEE/CVF Conference on Computer Vision and Pattern Recognition*, pages 8823–8833, 2022.
- [77] Linhui Li, Xuecheng Wang, Dongfang Yang, Yifan Ju, Zhongxu Zhang, and Jing Lian. Real-time heterogeneous road-agents trajectory prediction using hierarchical convolutional networks and multi-task learning. *IEEE Transactions on Intelligent Vehicles*, 2023.
- [78] Görkay Aydemir, Adil Kaan Akan, and Fatma Güney. Adapt: Efficient multi-agent trajectory prediction with adaptation. In *Proceedings of the IEEE/CVF International Conference on Computer Vision*, pages 8295–8305, 2023.
- [79] Pei Xu, Jean-Bernard Hayet, and Ioannis Karamouzas. Context-aware timewise vaes for real-time vehicle trajectory prediction. *IEEE Robotics and Automation Letters*, 8(9):5440–5447, 2023.
- [80] Daehee Park, Hobin Ryu, Yunseo Yang, Jegyeong Cho, Jiwon Kim, and Kuk-Jin Yoon. Leveraging future relationship reasoning for vehicle trajectory prediction. In *International Conference on Learning Representations (ICLR 2023)*. Eleventh International Conference on Learning Representations, 2023.
- [81] Pei Xu, Jean-Bernard Hayet, and Ioannis Karamouzas. Context-aware timewise vaes for real-time vehicle trajectory prediction. *IEEE Robotics and Automation Letters*, 8(9):5440–5447, 2023.
- [82] Sehwan Choi, Jungho Kim, Junyong Yun, and Jun Won Choi. R-pred: Two-stage motion prediction via tube-query attention-based trajectory refinement. In *Proceedings of the IEEE/CVF International Conference on Computer Vision*, pages 8525–8535, 2023.
- [83] Di Wen, Haoran Xu, Zhaocheng He, Zhe Wu, Guang Tan, and Peixi Peng. Density-adaptive model based on motif matrix for multi-agent trajectory prediction. In *Proceedings of the IEEE/CVF Conference on Computer Vision and Pattern Recognition*, pages 14822–14832, 2024.
- [84] Maximilian Schäfer, Kun Zhao, and Anton Kummert. Caspnet++: Joint multi-agent motion prediction. In 2024 IEEE Intelligent Vehicles Symposium (IV), pages 1294–1301. IEEE, 2024.
- [85] Xishun Wang, Tong Su, Fang Da, and Xiaodong Yang. Prophnet: Efficient agent-centric motion forecasting with anchor-informed proposals. In *Proceedings of the IEEE/CVF Conference on Computer Vision and Pattern Recognition*, pages 21995–22003, 2023.
- [86] Harsh Yadav, Maximilian Schaefer, Kun Zhao, and Tobias Meisen. Caspformer: Trajectory prediction from bev images with deformable attention. In *International Conference on Pattern Recognition*, pages 420–434. Springer, 2025.
- [87] Zikang Zhou, Jianping Wang, Yung-Hui Li, and Yu-Kai Huang. Query-centric trajectory prediction. In Proceedings of the IEEE/CVF Conference on Computer Vision and Pattern Recognition, pages 17863– 17873, 2023.
- [88] Jiquan Ngiam, Benjamin Caine, Vijay Vasudevan, Zhengdong Zhang, Hao-Tien Lewis Chiang, Jeffrey Ling, Rebecca Roelofs, Alex Bewley, Chenxi Liu, Ashish Venugopal, et al. Scene transformer: A unified architecture for predicting multiple agent trajectories. arXiv preprint arXiv:2106.08417, 2021.
- [89] Stepan Konev. Mpa: Multipath++ based architecture for motion prediction. *arXiv preprint arXiv:2206.10041*, 2022.
- [90] Zhiyu Huang, Xiaoyu Mo, and Chen Lv. Recoat: A deep learning-based framework for multi-modal motion prediction in autonomous driving application. In 2022 IEEE 25th International Conference on Intelligent Transportation Systems (ITSC), pages 988–993. IEEE, 2022.
- [91] Zhiyu Huang, Haochen Liu, Jingda Wu, and Chen Lv. Differentiable integrated motion prediction and planning with learnable cost function for autonomous driving. *IEEE transactions on neural networks and learning systems*, 2023.

- [92] Camiel Oerlemans, Bram Grooten, Michiel Braat, Alaa Alassi, Emilia Silvas, and Decebal Constantin Mocanu. Limtr: Time series motion prediction for diverse road users through multimodal feature integration. arXiv preprint arXiv:2410.15819, 2024.
- [93] Xiaosong Jia, Penghao Wu, Li Chen, Yu Liu, Hongyang Li, and Junchi Yan. Hdgt: Heterogeneous driving graph transformer for multi-agent trajectory prediction via scene encoding. *IEEE transactions on pattern analysis and machine intelligence*, 45(11):13860–13875, 2023.
- [94] Ari Seff, Brian Cera, Dian Chen, Mason Ng, Aurick Zhou, Nigamaa Nayakanti, Khaled S Refaat, Rami Al-Rfou, and Benjamin Sapp. Motionlm: Multi-agent motion forecasting as language modeling. In Proceedings of the IEEE/CVF International Conference on Computer Vision, pages 8579–8590, 2023.
- [95] Shaoshuai Shi, Li Jiang, Dengxin Dai, and Bernt Schiele. Mtr++: Multi-agent motion prediction with symmetric scene modeling and guided intention querying. *IEEE Transactions on Pattern Analysis and Machine Intelligence*, 46(5):3955–3971, 2024.
- [96] Xiaoji Zheng, Lixiu Wu, Zhijie Yan, Yuanrong Tang, Hao Zhao, Chen Zhong, Bokui Chen, and Jiangtao Gong. Large language models powered context-aware motion prediction in autonomous driving. In 2024 IEEE/RSJ International Conference on Intelligent Robots and Systems (IROS), pages 980–985. IEEE, 2024.
- [97] Jiawei Sun, Chengran Yuan, Shuo Sun, Shanze Wang, Yuhang Han, Shuailei Ma, Zefan Huang, Anthony Wong, Keng Peng Tee, and Marcelo H Ang. Controlmtr: Control-guided motion transformer with scenecompliant intention points for feasible motion prediction. In 2024 IEEE 27th International Conference on Intelligent Transportation Systems (ITSC), pages 1507–1514. IEEE, 2024.
- [98] Nejla Özmen and Esra Erkuş-Duman. On the poisson-charlier polynomials. *Serdica Mathematical Journal*, 41(4):457p–470p, 2015.
- [99] Margit Rösler. Generalized hermite polynomials and the heat equation for dunkl operators. *Communications in Mathematical Physics*, 192:519–542, 1998.
- [100] Yanjun Huang, Jiatong Du, Ziru Yang, Zewei Zhou, Lin Zhang, and Hong Chen. A survey on trajectory-prediction methods for autonomous driving. *IEEE Transactions on Intelligent Vehicles*, 7(3):652–674, 2022.
- [101] Thomas Batz, Kym Watson, and Jurgen Beyerer. Recognition of dangerous situations within a cooperative group of vehicles. In 2009 IEEE Intelligent Vehicles Symposium, pages 907–912. IEEE, 2009.
- [102] Mattias Brännström, Erik Coelingh, and Jonas Sjöberg. Model-based threat assessment for avoiding arbitrary vehicle collisions. *IEEE Transactions on Intelligent Transportation Systems*, 11(3):658–669, 2010.
- [103] Helgo Dyckmanns, Richard Matthaei, Markus Maurer, Bernd Lichte, Jan Effertz, and Dirk Stüker. Object tracking in urban intersections based on active use of a priori knowledge: Active interacting multi model filter. In 2011 IEEE Intelligent Vehicles Symposium (IV), pages 625–630. IEEE, 2011.
- [104] Vasileios Lefkopoulos, Marcel Menner, Alexander Domahidi, and Melanie N Zeilinger. Interaction-aware motion prediction for autonomous driving: A multiple model kalman filtering scheme. *IEEE Robotics* and Automation Letters, 6(1):80–87, 2020.
- [105] Yijing Wang, Zhengxuan Liu, Zhiqiang Zuo, Zheng Li, Li Wang, and Xiaoyuan Luo. Trajectory planning and safety assessment of autonomous vehicles based on motion prediction and model predictive control. *IEEE Transactions on Vehicular Technology*, 68(9):8546–8556, 2019.
- [106] Haoran Song, Di Luan, Wenchao Ding, Michael Y Wang, and Qifeng Chen. Learning to predict vehicle trajectories with model-based planning. In *Conference on Robot Learning*, pages 1035–1045. PMLR, 2022.
- [107] Quan Tran and Jonas Firl. Online maneuver recognition and multimodal trajectory prediction for intersection assistance using non-parametric regression. In 2014 ieee intelligent vehicles symposium proceedings, pages 918–923. IEEE, 2014.
- [108] Yuande Jiang, Bing Zhu, Shun Yang, Jian Zhao, and Weiwen Deng. Vehicle trajectory prediction considering driver uncertainty and vehicle dynamics based on dynamic bayesian network. *IEEE Transactions on Systems, Man, and Cybernetics: Systems*, 2022.

- [109] Samet Ayhan and Hanan Samet. Aircraft trajectory prediction made easy with predictive analytics. In Proceedings of the 22nd ACM SIGKDD International Conference on Knowledge Discovery and Data Mining, pages 21–30, 2016.
- [110] Zhibin Qiu, Jiangjun Ruan, Daochun Huang, Ziheng Pu, and Shengwen Shu. A prediction method for breakdown voltage of typical air gaps based on electric field features and support vector machine. *IEEE Transactions on Dielectrics and Electrical Insulation*, 22(4):2125–2135, 2015.
- [111] Matthias Schreier, Volker Willert, and Jürgen Adamy. An integrated approach to maneuver-based trajectory prediction and criticality assessment in arbitrary road environments. *IEEE Transactions on Intelligent Transportation Systems*, 17(10):2751–2766, 2016.
- [112] Junru Gu, Chen Sun, and Hang Zhao. Densetnt: End-to-end trajectory prediction from dense goal sets. In Proceedings of the IEEE/CVF International Conference on Computer Vision, pages 15303–15312, 2021.
- [113] Hashmatullah Sadid and Constantinos Antoniou. Dynamic spatio-temporal graph neural network for surrounding-aware trajectory prediction of autonomous vehicles. *IEEE Transactions on Intelligent Vehicles*, 2024.
- [114] DN Jagadish, Arun Chauhan, and Lakshman Mahto. Conditional variational autoencoder networks for autonomous vehicle path prediction. *Neural Processing Letters*, 54(5):3965–3978, 2022.
- [115] Zilai Zeng, Ce Zhang, Shijie Wang, and Chen Sun. Goal-conditioned predictive coding for offline reinforcement learning. Advances in Neural Information Processing Systems, 36, 2024.
- [116] Rushdi Alsaleh and Tarek Sayed. Modeling pedestrian-cyclist interactions in shared space using inverse reinforcement learning. *Transportation research part F: traffic psychology and behaviour*, 70:37–57, 2020.
- [117] Zan Yang, Wei Nai, Dan Li, Lu Liu, and Ziyu Chen. A mixed generative adversarial imitation learning based vehicle path planning algorithm. *IEEE Access*, 2024.
- [118] David Hilbert. Über die gleichung neunten grades. In *Algebra· Invariantentheorie Geometrie*, pages 393–400. Springer, 1970.
- [119] Ken-Ichi Funahashi. On the approximate realization of continuous mappings by neural networks. *Neural networks*, 2(3):183–192, 1989.
- [120] George Cybenko. Approximation by superpositions of a sigmoidal function. *Mathematics of control, signals and systems*, 2(4):303–314, 1989.
- [121] Kurt Hornik, Maxwell Stinchcombe, and Halbert White. Multilayer feedforward networks are universal approximators. *Neural networks*, 2(5):359–366, 1989.
- [122] Kurt Hornik. Approximation capabilities of multilayer feedforward networks. Neural networks, 4(2):251–257, 1991.
- [123] Shriyank Somvanshi, Syed Aaqib Javed, Md Monzurul Islam, Diwas Pandit, and Subasish Das. A survey on kolmogorov-arnold network. *arXiv preprint arXiv:2411.06078*, 2024.
- [124] Kexin Ma, Xu Lu, Bragazzi Luigi Nicola, and Biao Tang. Integrating kolmogorov-arnold networks with ordinary differential equations for efficient, interpretable and robust deep learning: A case study in the epidemiology of infectious diseases. *medRxiv*, pages 2024–09, 2024.
- [125] Alexander Dylan Bodner, Antonio Santiago Tepsich, Jack Natan Spolski, and Santiago Pourteau. Convolutional kolmogorov-arnold networks. arXiv preprint arXiv:2406.13155, 2024.
- [126] Zavareh Bozorgasl and Hao Chen. Wav-kan: Wavelet kolmogorov-arnold networks. *arXiv preprint arXiv:2405.12832*, 2024.
- [127] Cristian J Vaca-Rubio, Luis Blanco, Roberto Pereira, and Màrius Caus. Kolmogorov-arnold networks (kans) for time series analysis. *arXiv preprint arXiv:2405.08790*, 2024.
- [128] Ioannis E Livieris. C-kan: A new approach for integrating convolutional layers with kolmogorov–arnold networks for time-series forecasting. *Mathematics*, 12(19):3022, 2024.
- [129] Remi Genet and Hugo Inzirillo. Tkan: Temporal kolmogorov-arnold networks. *arXiv preprint* arXiv:2405.07344, 2024.

- [130] Glenn W Brier. Verification of forecasts expressed in terms of probability. *Monthly weather review*, 78(1):1–3, 1950.
- [131] A. N. Kolmogorov. On the best approximation of continuous functions. *Doklady Akademii Nauk SSSR*, 1947:Approximate page numbers if available, 1947.
- [132] P Billingsley. Probability and measure. 3rd wiley. New York, 1995.
- [133] Norman L Johnson, Adrienne W Kemp, and Samuel Kotz. Univariate discrete distributions, volume 444. John Wiley & Sons, 2005.
- [134] A. F. Timan. Theory of Approximation of Functions of a Real Variable, volume 34 of International Series of Monographs in Pure and Applied Mathematics. Pergamon Press, 1963.
- [135] William W Hager. Lipschitz continuity for constrained processes. SIAM Journal on Control and Optimization, 17(3):321–338, 1979.
- [136] JC Ferrando and LM Sánchez Ruiz. A survey on recent advances on the nikodým boundedness theorem and spaces of simple functions. *The Rocky Mountain Journal of Mathematics*, pages 139–172, 2004.
- [137] Andrew Alleyne. Improved vehicle performance using combined suspension and braking forces. *Vehicle System Dynamics*, 27(4):235–265, 1997.
- [138] Ksander N de Winkel, Tugrul Irmak, Riender Happee, and Barys Shyrokau. Standards for passenger comfort in automated vehicles: Acceleration and jerk. *Applied Ergonomics*, 106:103881, 2023.
- [139] Ram Venkataraman Iyer, Xiaobo Tan, and Perinkulam S Krishnaprasad. Approximate inversion of the preisach hysteresis operator with application to control of smart actuators. *IEEE Transactions on automatic control*, 50(6):798–810, 2005.
- [140] Gordon Frank Newell. A simplified car-following theory: a lower order model. *Transportation Research Part B: Methodological*, 36(3):195–205, 2002.
- [141] Zhen Yao, Xin Li, Bo Lang, and Mooi Choo Chuah. Goal-lbp: Goal-based local behavior guided trajectory prediction for autonomous driving. *IEEE Transactions on Intelligent Transportation Systems*, 2023.
- [142] Peter G Gipps. A behavioural car-following model for computer simulation. *Transportation research part B: methodological*, 15(2):105–111, 1981.
- [143] Antoine Ayache and Jacques Lévy Véhel. On the identification of the pointwise hölder exponent of the generalized multifractional brownian motion. Stochastic Processes and their Applications, 111(1):119– 156, 2004.
- [144] Anupriya Vysala and Joseph Gomes. Evaluating and validating cluster results. *arXiv preprint* arXiv:2007.08034, 2020.
- [145] Mingqian Li, Panrong Tong, Mo Li, Zhongming Jin, Jianqiang Huang, and Xian-Sheng Hua. Traffic flow prediction with vehicle trajectories. In *Proceedings of the AAAI Conference on Artificial Intelligence*, volume 35, pages 294–302, 2021.
- [146] Xiaoyu Mo, Zhiyu Huang, Yang Xing, and Chen Lv. Multi-agent trajectory prediction with heterogeneous edge-enhanced graph attention network. *IEEE Transactions on Intelligent Transportation Systems*, 23(7):9554–9567, 2022.
- [147] Lan Feng, Mohammadhossein Bahari, Kaouther Messaoud Ben Amor, Éloi Zablocki, Matthieu Cord, and Alexandre Alahi. Unitraj: A unified framework for scalable vehicle trajectory prediction. In European Conference on Computer Vision, pages 106–123. Springer, 2024.
- [148] Andreas Geiger, Philip Lenz, and Raquel Urtasun. Are we ready for autonomous driving? the kitti vision benchmark suite. In 2012 IEEE conference on computer vision and pattern recognition, pages 3354–3361. IEEE, 2012.
- [149] Xinyu Huang, Xinjing Cheng, Qichuan Geng, Binbin Cao, Dingfu Zhou, Peng Wang, Yuanqing Lin, and Ruigang Yang. The apolloscape dataset for autonomous driving. In *Proceedings of the IEEE conference* on computer vision and pattern recognition workshops, pages 954–960, 2018.
- [150] Wei Zhan, Liting Sun, Di Wang, Haojie Shi, Aubrey Clausse, Maximilian Naumann, Julius Kummerle, Hendrik Konigshof, Christoph Stiller, Arnaud de La Fortelle, et al. Interaction dataset: An international, adversarial and cooperative motion dataset in interactive driving scenarios with semantic maps. arXiv preprint arXiv:1910.03088, 2019.

- [151] Julian Bock, Robert Krajewski, Tobias Moers, Steffen Runde, Lennart Vater, and Lutz Eckstein. The ind dataset: A drone dataset of naturalistic road user trajectories at german intersections. In 2020 IEEE Intelligent Vehicles Symposium (IV), pages 1929–1934. IEEE, 2020.
- [152] Robert Krajewski, Tobias Moers, Julian Bock, Lennart Vater, and Lutz Eckstein. The round dataset: A drone dataset of road user trajectories at roundabouts in germany. In 2020 IEEE 23rd International Conference on Intelligent Transportation Systems (ITSC), pages 1–6, 2020.
- [153] Robert Krajewski, Julian Bock, Laurent Kloeker, and Lutz Eckstein. The highd dataset: A drone dataset of naturalistic vehicle trajectories on german highways for validation of highly automated driving systems. In 2018 21st international conference on intelligent transportation systems (ITSC), pages 2118–2125. IEEE, 2018.



The diagram illustrates of three driving styles: Conservative, Aggressive and Normal (CAN), with their corresponding trajectories represented by lines recorded at each time step. The lengths of the lines indicate the driving distance, while the direction is shown by arrows. Conservative drivers typically move at low speeds or stop to avoid obstacles. Aggressive drivers often travel at high speeds and are prone to overtaking other vehicles. Normal drivers maintain a constant speed and frequently change lanes to ensure safety.

#### **NeurIPS Paper Checklist**

#### 1. Claims

Question: Do the main claims made in the abstract and introduction accurately reflect the paper's contributions and scope?

Answer: [Yes].

Justification: The main claims illustrate in Figure 1 in Section 1 (introduction). Our main contributions in this paper are summarized as follows:

- To handle the vehicle trajectory prediction task, we propose for the first time a novel Driving-Style-Adaptive (DSA) framework tailored to the **driving styles** of human drivers, effectively leverages trajectory information.
- We utilize polynomial approximation operators to approximate and predict trajectories under different driving styles: Conservative, Aggressive and Normal (CAN). These operators support a mathematical explanation matching mechanism between driving style with a corresponding polynomial form.
- The experimental results on the real-world datasets (nuScenes, Argoverse and Waymo) demonstrate that our model significantly outperforms existing methods in vehicle trajectory prediction.

#### Guidelines:

- The answer NA means that the abstract and introduction do not include the claims made in the paper.
- The abstract and/or introduction should clearly state the claims made, including the contributions
  made in the paper and important assumptions and limitations. A No or NA answer to this
  question will not be perceived well by the reviewers.
- The claims made should match theoretical and experimental results, and reflect how much the results can be expected to generalize to other settings.
- It is fine to include aspirational goals as motivation as long as it is clear that these goals are not attained by the paper.

#### 2. Limitations

Question: Does the paper discuss the limitations of the work performed by the authors?

Answer: [Yes].

Justification: We discuss the limitation in Appendix.

#### Guidelines:

- The answer NA means that the paper has no limitation while the answer No means that the paper has limitations, but those are not discussed in the paper.
- The authors are encouraged to create a separate "Limitations" section in their paper.

- The paper should point out any strong assumptions and how robust the results are to violations of these assumptions (e.g., independence assumptions, noiseless settings, model well-specification, asymptotic approximations only holding locally). The authors should reflect on how these assumptions might be violated in practice and what the implications would be.
- The authors should reflect on the scope of the claims made, e.g., if the approach was only tested on a few datasets or with a few runs. In general, empirical results often depend on implicit assumptions, which should be articulated.
- The authors should reflect on the factors that influence the performance of the approach. For example, a facial recognition algorithm may perform poorly when image resolution is low or images are taken in low lighting. Or a speech-to-text system might not be used reliably to provide closed captions for online lectures because it fails to handle technical jargon.
- The authors should discuss the computational efficiency of the proposed algorithms and how
  they scale with dataset size.
- If applicable, the authors should discuss possible limitations of their approach to address problems
  of privacy and fairness.
- While the authors might fear that complete honesty about limitations might be used by reviewers
  as grounds for rejection, a worse outcome might be that reviewers discover limitations that
  aren't acknowledged in the paper. The authors should use their best judgment and recognize
  that individual actions in favor of transparency play an important role in developing norms that
  preserve the integrity of the community. Reviewers will be specifically instructed to not penalize
  honesty concerning limitations.

#### 3. Theory assumptions and proofs

Question: For each theoretical result, does the paper provide the full set of assumptions and a complete (and correct) proof?

Answer: [Yes].

Justification: We provide the mathematics properties for matching driving style and corresponding polynomial in Section 3.2, for full proof is in Appendix C.

#### Guidelines:

- The answer NA means that the paper does not include theoretical results.
- All the theorems, formulas, and proofs in the paper should be numbered and cross-referenced.
- All assumptions should be clearly stated or referenced in the statement of any theorems.
- The proofs can either appear in the main paper or the supplemental material, but if they appear in the supplemental material, the authors are encouraged to provide a short proof sketch to provide intuition.
- Inversely, any informal proof provided in the core of the paper should be complemented by formal proofs provided in appendix or supplemental material.
- Theorems and Lemmas that the proof relies upon should be properly referenced.

#### 4. Experimental result reproducibility

Question: Does the paper fully disclose all the information needed to reproduce the main experimental results of the paper to the extent that it affects the main claims and/or conclusions of the paper (regardless of whether the code and data are provided or not)?

Answer: [Yes].

Justification: Please refer to Section 3.3.1, 3.3.2 and the released codes in supplemental material.

#### Guidelines:

- The answer NA means that the paper does not include experiments.
- If the paper includes experiments, a No answer to this question will not be perceived well by the reviewers: Making the paper reproducible is important, regardless of whether the code and data are provided or not.
- If the contribution is a dataset and/or model, the authors should describe the steps taken to make their results reproducible or verifiable.
- Depending on the contribution, reproducibility can be accomplished in various ways. For example, if the contribution is a novel architecture, describing the architecture fully might suffice, or if the contribution is a specific model and empirical evaluation, it may be necessary to either make it possible for others to replicate the model with the same dataset, or provide access to the model. In general, releasing code and data is often one good way to accomplish this, but reproducibility can also be provided via detailed instructions for how to replicate the results, access to a hosted model (e.g., in the case of a large language model), releasing of a model checkpoint, or other means that are appropriate to the research performed.

- While NeurIPS does not require releasing code, the conference does require all submissions
  to provide some reasonable avenue for reproducibility, which may depend on the nature of the
  contribution. For example
  - (a) If the contribution is primarily a new algorithm, the paper should make it clear how to reproduce that algorithm.
  - (b) If the contribution is primarily a new model architecture, the paper should describe the architecture clearly and fully.
  - (c) If the contribution is a new model (e.g., a large language model), then there should either be a way to access this model for reproducing the results or a way to reproduce the model (e.g., with an open-source dataset or instructions for how to construct the dataset).
  - (d) We recognize that reproducibility may be tricky in some cases, in which case authors are welcome to describe the particular way they provide for reproducibility. In the case of closed-source models, it may be that access to the model is limited in some way (e.g., to registered users), but it should be possible for other researchers to have some path to reproducing or verifying the results.

#### 5. Open access to data and code

Question: Does the paper provide open access to the data and code, with sufficient instructions to faithfully reproduce the main experimental results, as described in supplemental material?

Answer: [Yes].

Justification: We provide the code in supplemental material.

#### Guidelines:

- The answer NA means that paper does not include experiments requiring code.
- Please see the NeurIPS code and data submission guidelines (https://nips.cc/public/guides/CodeSubmissionPolicy) for more details.
- While we encourage the release of code and data, we understand that this might not be possible, so "No" is an acceptable answer. Papers cannot be rejected simply for not including code, unless this is central to the contribution (e.g., for a new open-source benchmark).
- The instructions should contain the exact command and environment needed to run to reproduce
  the results. See the NeurIPS code and data submission guidelines (https://nips.cc/public/
  guides/CodeSubmissionPolicy) for more details.
- The authors should provide instructions on data access and preparation, including how to access the raw data, preprocessed data, intermediate data, and generated data, etc.
- The authors should provide scripts to reproduce all experimental results for the new proposed method and baselines. If only a subset of experiments are reproducible, they should state which ones are omitted from the script and why.
- At submission time, to preserve anonymity, the authors should release anonymized versions (if applicable).
- Providing as much information as possible in supplemental material (appended to the paper) is recommended, but including URLs to data and code is permitted.

#### 6. Experimental setting/details

Question: Does the paper specify all the training and test details (e.g., data splits, hyperparameters, how they were chosen, type of optimizer, etc.) necessary to understand the results?

Answer: [Yes].

Justification: We detail are in Section 3.3.2.

#### Guidelines:

- The answer NA means that the paper does not include experiments.
- The experimental setting should be presented in the core of the paper to a level of detail that is necessary to appreciate the results and make sense of them.
- The full details can be provided either with the code, in appendix, or as supplemental material.

#### 7. Experiment statistical significance

Question: Does the paper report error bars suitably and correctly defined or other appropriate information about the statistical significance of the experiments?

Answer: [No].

Justification: This paper does not report error bars following the practice of previous work [70, 71, 88]. Guidelines:

• The answer NA means that the paper does not include experiments.

- The authors should answer "Yes" if the results are accompanied by error bars, confidence intervals, or statistical significance tests, at least for the experiments that support the main claims of the paper.
- The factors of variability that the error bars are capturing should be clearly stated (for example, train/test split, initialization, random drawing of some parameter, or overall run with given experimental conditions).
- The method for calculating the error bars should be explained (closed form formula, call to a library function, bootstrap, etc.)
- The assumptions made should be given (e.g., Normally distributed errors).
- It should be clear whether the error bar is the standard deviation or the standard error of the mean.
- It is OK to report 1-sigma error bars, but one should state it. The authors should preferably report
  a 2-sigma error bar than state that they have a 96% CI, if the hypothesis of Normality of errors is
  not verified.
- For asymmetric distributions, the authors should be careful not to show in tables or figures symmetric error bars that would yield results that are out of range (e.g. negative error rates).
- If error bars are reported in tables or plots, The authors should explain in the text how they were calculated and reference the corresponding figures or tables in the text.

#### 8. Experiments compute resources

Question: For each experiment, does the paper provide sufficient information on the computer resources (type of compute workers, memory, time of execution) needed to reproduce the experiments?

Answer: [Yes]

Justification: Please refer to Section 4.2.1 and Section 4.3.

#### Guidelines:

- The answer NA means that the paper does not include experiments.
- The paper should indicate the type of compute workers CPU or GPU, internal cluster, or cloud provider, including relevant memory and storage.
- The paper should provide the amount of compute required for each of the individual experimental runs as well as estimate the total compute.
- The paper should disclose whether the full research project required more compute than the experiments reported in the paper (e.g., preliminary or failed experiments that didn't make it into the paper).

#### 9. Code of ethics

Question: Does the research conducted in the paper conform, in every respect, with the NeurIPS Code of Ethics https://neurips.cc/public/EthicsGuidelines?

Answer: [Yes] .

Justification: This paper conforms with the NeurIPS Code of Ethics.

#### Guidelines:

- The answer NA means that the authors have not reviewed the NeurIPS Code of Ethics.
- If the authors answer No, they should explain the special circumstances that require a deviation from the Code of Ethics.
- The authors should make sure to preserve anonymity (e.g., if there is a special consideration due to laws or regulations in their jurisdiction).

#### 10. Broader impacts

Question: Does the paper discuss both potential positive societal impacts and negative societal impacts of the work performed?

Answer: [NA].

Justification: There is no societal impact of the work performed.

#### Guidelines:

- The answer NA means that there is no societal impact of the work performed.
- If the authors answer NA or No, they should explain why their work has no societal impact or why the paper does not address societal impact.
- Examples of negative societal impacts include potential malicious or unintended uses (e.g., disinformation, generating fake profiles, surveillance), fairness considerations (e.g., deployment of technologies that could make decisions that unfairly impact specific groups), privacy considerations, and security considerations.

- The conference expects that many papers will be foundational research and not tied to particular applications, let alone deployments. However, if there is a direct path to any negative applications, the authors should point it out. For example, it is legitimate to point out that an improvement in the quality of generative models could be used to generate deepfakes for disinformation. On the other hand, it is not needed to point out that a generic algorithm for optimizing neural networks could enable people to train models that generate Deepfakes faster.
- The authors should consider possible harms that could arise when the technology is being used
  as intended and functioning correctly, harms that could arise when the technology is being used
  as intended but gives incorrect results, and harms following from (intentional or unintentional)
  misuse of the technology.
- If there are negative societal impacts, the authors could also discuss possible mitigation strategies
  (e.g., gated release of models, providing defenses in addition to attacks, mechanisms for monitoring misuse, mechanisms to monitor how a system learns from feedback over time, improving the
  efficiency and accessibility of ML).

#### 11. Safeguards

Question: Does the paper describe safeguards that have been put in place for responsible release of data or models that have a high risk for misuse (e.g., pretrained language models, image generators, or scraped datasets)?

Answer: [NA].

Justification: This paper poses no such risks.

#### Guidelines:

- The answer NA means that the paper poses no such risks.
- Released models that have a high risk for misuse or dual-use should be released with necessary
  safeguards to allow for controlled use of the model, for example by requiring that users adhere to
  usage guidelines or restrictions to access the model or implementing safety filters.
- Datasets that have been scraped from the Internet could pose safety risks. The authors should describe how they avoided releasing unsafe images.
- We recognize that providing effective safeguards is challenging, and many papers do not require this, but we encourage authors to take this into account and make a best faith effort.

#### 12. Licenses for existing assets

Question: Are the creators or original owners of assets (e.g., code, data, models), used in the paper, properly credited and are the license and terms of use explicitly mentioned and properly respected?

Answer: [Yes].

Justification: We cite the datasets we use in Section 4.1 and introduce them in Section B.1.

#### Guidelines:

- The answer NA means that the paper does not use existing assets.
- The authors should cite the original paper that produced the code package or dataset.
- The authors should state which version of the asset is used and, if possible, include a URL.
- The name of the license (e.g., CC-BY 4.0) should be included for each asset.
- For scraped data from a particular source (e.g., website), the copyright and terms of service of that source should be provided.
- If assets are released, the license, copyright information, and terms of use in the package should
  be provided. For popular datasets, paperswithcode.com/datasets has curated licenses for
  some datasets. Their licensing guide can help determine the license of a dataset.
- For existing datasets that are re-packaged, both the original license and the license of the derived asset (if it has changed) should be provided.
- If this information is not available online, the authors are encouraged to reach out to the asset's creators.

#### 13. New assets

Question: Are new assets introduced in the paper well documented and is the documentation provided alongside the assets?

Answer: [Yes].

Justification: We provide it in the supplemental material.

#### Guidelines:

• The answer NA means that the paper does not release new assets.

- Researchers should communicate the details of the dataset/code/model as part of their submissions via structured templates. This includes details about training, license, limitations, etc.
- The paper should discuss whether and how consent was obtained from people whose asset is used.
- At submission time, remember to anonymize your assets (if applicable). You can either create an
  anonymized URL or include an anonymized zip file.

#### 14. Crowdsourcing and research with human subjects

Question: For crowdsourcing experiments and research with human subjects, does the paper include the full text of instructions given to participants and screenshots, if applicable, as well as details about compensation (if any)?

Answer: [NA].

Justification: The paper does not involve crowdsourcing nor research with human subjects.

#### Guidelines:

- The answer NA means that the paper does not involve crowdsourcing nor research with human subjects.
- Including this information in the supplemental material is fine, but if the main contribution of the
  paper involves human subjects, then as much detail as possible should be included in the main
  paper.
- According to the NeurIPS Code of Ethics, workers involved in data collection, curation, or other labor should be paid at least the minimum wage in the country of the data collector.

#### 15. Institutional review board (IRB) approvals or equivalent for research with human subjects

Question: Does the paper describe potential risks incurred by study participants, whether such risks were disclosed to the subjects, and whether Institutional Review Board (IRB) approvals (or an equivalent approval/review based on the requirements of your country or institution) were obtained?

Answer: [NA].

Justification: This paper does not involve crowdsourcing nor research with human subjects.

#### Guidelines:

- The answer NA means that the paper does not involve crowdsourcing nor research with human subjects.
- Depending on the country in which research is conducted, IRB approval (or equivalent) may be required for any human subjects research. If you obtained IRB approval, you should clearly state this in the paper.
- We recognize that the procedures for this may vary significantly between institutions and locations, and we expect authors to adhere to the NeurIPS Code of Ethics and the guidelines for their institution.
- For initial submissions, do not include any information that would break anonymity (if applicable), such as the institution conducting the review.

#### 16. Declaration of LLM usage

Question: Does the paper describe the usage of LLMs if it is an important, original, or non-standard component of the core methods in this research? Note that if the LLM is used only for writing, editing, or formatting purposes and does not impact the core methodology, scientific rigorousness, or originality of the research, declaration is not required.

Answer: [NA].

Justification: The core method development in this research does not involve LLMs as any important, original or non-standard components

#### Guidelines:

- The answer NA means that the core method development in this research does not involve LLMs as any important, original, or non-standard components.
- Please refer to our LLM policy (https://neurips.cc/Conferences/2025/LLM) for what should or should not be described.

### Appendix of A Driving-Style-Adaptive Framework for Vehicle Trajectory Prediction

#### A Problem Background

#### A.1 Vehicle Trajectory Prediction

The methods for vehicle trajectory prediction can be broadly classified into four categories [100]. These include: (i) Physics-based methods: These employ vehicle dynamics or kinematics models, such as singles trajectory methods, Monte Carlo, and Kalman filtering methods [101, 102, 103, 104, 105, 106]. These methods are known for their conciseness, efficiency, and computational effectiveness. (ii) Classic machine learning: Unlike physics-based methods that rely on several physics models, classic machine learning approaches apply data-driven models and consider additional factors for predicting trajectories. Examples include the Hidden Markov Model, Dynamic Bayesian Network, and K-Nearest Neighbors [107, 108, 109, 110, 111]. However, these traditional methods are typically only suitable for simple prediction scenarios and short-term prediction tasks.

Recently, with the advancement of modern machine learning, vehicle trajectory prediction methods based on: (iii) Deep learning and (iv) Reinforcement learning become increasingly popular. These methods are capable of considering interaction-related factors, understanding high-dimensional complex policies, and adapting to more complex scenarios. Examples include Graph Convolutional Network, Graph Attention Network, Conditional Variational Auto Encoder, and reinforcement learning techniques such as Inverse Reinforcement Learning, Generative Adversarial Imitation Learning, and Deep IRL [112, 113, 83, 114, 115, 116, 117].

In summary, an increasing number of autonomous vehicle trials are utilizing deep learning or reinforcement learning methods to predict future vehicle trajectories. These approaches leverage expert demonstrations and extract interaction information from traffic participants and road conditions, considering a broader range of influencing factors.

#### A.2 Kolmogorov-Arnold Networks (KANs)

Hilbert's 13th problem [118] famously posits that it is impossible to solve general seventh-degree equations using only functions of two variables. Subsequent research by Kolmogorov et al.[36] has shown that any function involving multiple variables can be represented using a finite number of three-variable functions. Further studies as detailed by Arnol'd et al. [37], establish that even functions of just two variables are sufficient, as described in Theorem 2.1 presents significant for machine learning: learning a high-dimensional function essentially reduces to learning a limited number of one-dimensional basis functions  $\psi(x)$  in Equation (2).

In reference [20], the authors introduce Kolmogorov-Arnold Networks (KANs), which are neural network applications based on Theorem 2.1. Unlike Multi-Layer Perceptrons (MLPs) that founded on the universal approximation theorem [119, 120, 121, 122], KANs feature learnable activation functions on what are traditionally referred to as "edges" (neurons) and they utilize fixed activation functions at what are typically called "nodes" (weights). Uniquely, each weight in KANs is replaced by a univariate function parametrized as a spline, meaning the network contains no linear weights whatsoever.

A variety of KANs are used across different tasks as noted in [123], such as solving ordinary differential equations [44, 124], image classification and reconstruction [125, 126], and time series forecasting [127, 128, 129], among others. These applications demonstrate competitive or superior performance in efficiency and predictive power compared to traditional models. However, to the best of our knowledge, we are the first to utilize KANs in vehicle trajectory prediction. This involves approximating and predicting trajectories for different driving styles, expanding the range of basis functions, and providing explanations for specific matches between functions and trajectories.

#### **B** Dataset Information

#### **B.1** Datasets

We preprocess the three datasets using the official pip packages provided by their respective baselines. The characteristics of each dataset are summarized in Table 7.

Table 7: Characteristics of the evaluation datasets.

Datasets	Collect	Size	Library	Select
Argoverse [68]	Miami and Pittsburgh	23.69G	Argoverse API / devkit	Motion Forecasting
nuScenes [67]	Boston and Singapore	4.81G	nuscenes-devkit	Motional-Full dataset
Waymo [69]	Phoenix, AZ, Kirkland etc.	83.50G	waymo-open-dataset	Motion1.1-scenario

**nuScenes** This dataset [67] offers high-definition maps and trajectory data from 1,000 driving scenes in Boston and Singapore, areas noted for dense traffic and complex driving challenges. It comprises 245,414 trajectory instances, each a sequence of 2D coordinates over 8 seconds, sampled at 2Hz. The nuScenes benchmark requires predicting a target agent's 6-second future trajectory from a 2-second historical trajectory. The comprehensive dataset features approximately 1.4 million camera images, 390,000 LIDAR sweeps, 1.4 million RADAR sweeps, and 1.4 million object bounding boxes across 40,000 keyframes.

**Argoverse** This dataset [68] facilitates research in 3D tracking and motion forecasting for autonomous vehicles. Originating from select areas in Miami and Pittsburgh, it includes 113 scenes with 3D tracking annotations, featuring 324,557 significant vehicle trajectories derived from over 1,000 hours of driving. The forecasting component of Argoverse provides agent trajectories and high-definition maps, requiring the prediction of a target vehicle's future trajectory for the next 3 seconds, based on its past trajectory over two seconds, sampled at 10Hz. The dataset encompasses 333K real-world driving sequences, primarily at intersections or within dense traffic, each focusing on one target vehicle for trajectory prediction.

**Waymo** This dataset [69] publicly to aid the research community in investigating a wide range of interesting aspects of machine perception and autonomous driving technology. This Dataset we use is the Motion part, with object trajectories and corresponding 3D maps for 103,354 segments. Given agents' tracks for the past 1 second on a corresponding map, predict the joint future positions of 2 interacting agents for 8 seconds into the future. The ground truth future data for the interactive test set is hidden from challenge participants. The validation sets contain the ground truth future data for use in model development. In addition, the test and validation sets provide 2 interacting object tracks in the scene to be predicted.

#### **B.2** Metrics

We evaluate the predicted trajectory  $Y^t$  against the ground truth trajectory  $Y^t_{GT}$  using standard error-based metrics. Our DSA framework adopts the commonly used Average Displacement Error (ADE) and Final Displacement Error (FDE), as defined in [23]:

$$ADE = \frac{1}{T} \sum_{t=1}^{T} ||Y^t - Y_{GT}^t||_{L^2}, \text{ FDE} = ||Y^t - Y_{GT}^t||_{L^2}.$$

Here, the superscript t denotes the current time step, and T refers to the total number of time steps in the prediction horizon. The metrics we use include  $ADE_k$ ,  $FDE_k$ , minADE, minFDE, and b-minFDE. The subscript k indicates the Top-k most likely predicted future trajectories. The "min" variants (minADE and minFDE) compute the  $L^2$  distance between  $Y_{GT}^t$  and the closest predicted trajectory  $Y^t$  across all generated samples, averaged over all agents. The b-minFDE metric extends minFDE by incorporating the Brier score [130], which evaluates the calibration of the predictive distribution. It is defined as the sum of the Brier score and minFDE.

#### C Proof of Bound

As we discuss in Section 3.3.2, Kolmogorov's theorem [131] provides error bounds by evaluating the absolute value of the function and the overall variation in the function value. This is illustrated as follows:

**Theorem C.1** (Kolmogorov Theorem) For  $f \in C[a, b]$ , there exists a polynomial  $p_n$  such that approximation error is bounded by:

$$||f - p_n||_{L^{\infty}} \lesssim \left(\frac{\log n}{n}\right) V(f, [a, b]),$$

where V(f, [a, b]) denotes the total variation <sup>9</sup> of f over the interval.

From this theorem, we conclude that when n > e, increasing the degree n of  $p_n$  results in a smaller decrease in the theoretical upper bound on the approximation error.

However, in practice, considering computational cost and time, the value of n cannot be arbitrarily large. In this section, we provide three proofs corresponding to the three categories of drivers, demonstrating that under a given error limit  $\delta$ , there exists a relationship between the minimum degree n and the components of the trajectory to be approximated, as described in Section 2.1 (i.e., position (x, y), velocity, and acceleration). For clarity, we use f to represent each continuous component with respect to t.

#### C.1 Conservative Drives: Bernstein Polynomial

In Section 3.2.1, we use the properties of Bernstein polynomials  $(B_n)$  for their uniform convergence to approximate the trajectories of conservative drivers, characterized by low speed and minimal motion changes. The minimum degree n of the  $B_n$  polynomial is obtained by:

**Theorem C.2** For all  $\epsilon > 0$ , if  $\partial [B_n(f)] = n$ , then for a given error limit  $\delta$  with  $0 < \epsilon \le \delta \ll \infty$ , then  $n \ge \max |f''(\xi)| / 8\delta$ .

*Proof:* First, we calculate the error between f(x) and  $B_n(f)$ 

$$|f(x) - B_n(f)|$$

$$= \left| \sum_{k=0}^n \left[ f(x) - f\left(\frac{k}{n}\right) \right] \binom{n}{k} x^k (1-x)^{n-k} \right|$$

$$\leq \left| \sum_{k=0}^n \left[ -f''(\frac{k}{n}-x) - \frac{1}{2} f''\left(\frac{k}{n}-x\right)^2 \right] \cdot P_B(k) \right|$$

$$= \frac{1}{2} f''(\xi) \sum_{k=0}^n \left( \frac{n}{k} - x \right)^2 P_B(k) \qquad \xi \in \left(x, \frac{k}{n}\right). \tag{5}$$

In formula (4),  $P_B(k) \triangleq C_n^k x^k (1-x)^{n-k}$ . From Equation (5), we next proceed to prove

1. 
$$\sum_{k} \left( \frac{n}{k} - x \right) \cdot P_B(k) = 0$$

2. 
$$\sum_{k} \left( \frac{n}{k} - x \right)^{2} \cdot P_{B}(k) = \frac{x}{n} (1 - x)$$
.

For Equation 1, applying the Central Limit Theorem (CLT) as discussed in [132], we consider the total difference of weights, represented by [(n/k) - x]. Specifically, the probability p satisfies p = x = k/n. In this case, as described in [133], we have E(k) = nx. Thus, we can derive the expectation as follows:

$$E\left(\frac{k}{n}\right) = \frac{E\left(k\right)}{n} = x. \tag{6}$$

Therefore, Equation 1 simplifies to E(k/n) - x = 0.

For Equation 2, we employ a similar method; here  $(\frac{n}{k} - x)^2$  represents the squared difference in weights between  $\frac{k}{n}$  and x, alternatively described as the deviation between observation and expectation. According to Equation (6),

$$D\left(\frac{k}{n}\right) = \frac{nx}{n^2} \cdot (1-x) = \frac{x(1-x)}{n}.$$

<sup>&</sup>lt;sup>9</sup>**Total Variation** A measure of the total amount of variation in a function over a given interval [a,b], which is defined by  $\sup_{x\neq y}|f(x)-f(y)|/|x-y|$ .

Equation 2 corresponds to the squared deviation  $\left(\frac{n}{k}-x\right)^2$  based on weights  $P_B(k)$ . Moreover

$$\therefore E\left[\left(\frac{k}{n} - x\right)^2\right] = D\left(\frac{k}{n}\right),$$

$$\therefore (5) = \frac{1}{2}f''(\xi) \frac{x(1-x)}{n} \leqslant \frac{M_2}{8n}, \text{ with } M_2 = \max_{\xi \in \mathbb{D}} f''(\xi).$$

Considering the error limit  $\delta$ , we have:

$$\frac{M_2}{8n} < \delta \Rightarrow n \geqslant \frac{M_2}{8\delta}.$$

**Theorem C.3** If  $f \in L^p[a,b]$ ,  $B_n^{\omega}(f) \in [a,b]$  and  $\partial [B_n^{\omega}(f)] = n$ . For all  $\epsilon > 0$ ,  $0 < \epsilon \leqslant \delta \ll \infty$ ,  $\delta$  is given error limitation, then:

$$n \geqslant \frac{\max[|f''(\widetilde{\xi}) \cdot \omega|] \cdot (b-a)^2}{8\delta},$$
 where  $\omega$  is the weights of weighted  $B_n$  polynomials  $B_n^{\omega}(f)$ .

Here the error is  $L^{\infty}$  norm, the definition of  $B_n^{\omega}(f)$  is Proof:

$$B_n^{\omega}(f) = \sum_{k=0}^n f\left(\frac{k}{n}\right) \omega\left(\frac{k}{n}\right) \binom{n}{k} x^k (1-x)^{n-k}$$

Let u = (x - a) / (b - a), then  $u \in [0, 1]$ . So  $\widetilde{M}_2$  is similar to Theorem C.2, here

$$\widetilde{M}_{2} = \max_{u \in [0,1]} |g''(u)| = (b-a)^{2} |f''(\xi)|,$$

where  $g(u) = f\left(\frac{u-a}{b-a}\right)$ . The next following prove is similar to Theorem C.2.

#### C.2 Aggressive Drivers: Chebyshev Polynomial

In Section 3.2.2, aggressive drivers' trajectories are characterized by non-smooth, high-speed movements during motion changes. We use the Chebyshev polynomials  $T_n^c$  and their minimum-maximum error properties to approximate these trajectories. The minimum degree n of  $T_n^c$  polynomial is obtained as follows:

**Theorem C.4** For  $f \in L^p[a,b]$  and a given error bound  $\delta$  (where  $0 < \epsilon \le \delta \ll \infty$ ), the condition  $\partial [T_n^c(f)] =$ n is satisfied:

$$n \geqslant \frac{1}{\omega^{-1}\left(f, \frac{\delta}{12}\right)},\tag{7}$$

where  $\omega^{-1}$  is the inverse of the modulus of continuity for the function f.

To provide the proof of Theorem C.4, we first introduce the definition of the modulus of continuity and a lemma related to this proof.

**Definition C.5** (Modulus of Continuity in  $L^p$  Space) Let  $f \in L^p[a,b]$ ,  $p \ge 1$  and  $0 \le m \le b-a$ . The modulus of continuity  $\omega_p(m, f)$  is defined as:

$$\omega_{p}(m) = \omega_{p}(m, f)$$

$$= \sup_{0 \le h \le m} \left( \int_{a}^{b-h} |f(x+h) - f(x)|^{p} \right)^{1/p}$$

which represents the continuity norm for f over the interval [a, b].

For  $T_n^c$  polynomials belonging to the  $C_{2\pi}$  space  $^{10}$ , we use  $E_n(f)$  to denote the deviation of the approximation of f by a trigonometric polynomial  $T_n$  of degree n, as follow:

$$E_n(f) = \inf_{\{T_n\}} ||f - T_n||.$$

This deviation satisfies:

$$\parallel f \parallel = \sup_{-\pi \leqslant x \leqslant \pi} \mid f(x) \mid.$$

We call the above set the  $C_{2\pi}$  space

 $<sup>^{10}</sup>C_{2\pi}$  Space Let  $f \in \mathbb{R}$  with period  $2\pi$ . Define

**Lemma C.6** (Jackson [134]) Let  $f \in C_{2\pi}$ , then for all  $n \in \mathbb{N}$ , the following inequality holds:

$$E_n(f) \leqslant 12 \cdot \omega\left(f, \frac{1}{n}\right).$$

It is evident that  $T_n^c \subseteq C_{2\pi}$ . Based on Lemma C.6, we present the proof of Theorem C.4.

*Proof:* According to the definition of  $\delta$ , we have  $\parallel f - T_n \parallel_{L^{\infty}} < \delta$ . Lemma C.6 provides the modulus of continuity under the  $L^{\infty}$  space, so we need to relate  $\omega_p$  from Definition C.5 to  $\omega$  in Lemma C.6, which relates the  $L^p$  and  $L^{\infty}$  norms:

$$||g||_{L^p([a,b-h])} \le (b-a-h)^{\frac{1}{p}} \cdot ||g||_{L^{\infty}([a,b-h])}.$$

For the function difference g(x) = f(x+h) - f(x):

$$|f(x+h) - f(x)| \le \omega(f,h), \text{ for } \forall x \in [a,b-h].$$

Therefore, the  $\omega_p(m, f)$  is related to  $\omega(f, h)$  as follows:

$$\omega_p(h, f) \leqslant \left\{ \int_a^{b-h} \left[ \omega(f, h) \right]^p \right\}^{1/p}$$

$$= \omega(f, h) \cdot (b - a - h)^{\frac{1}{p}}.$$
(8)

When  $h \to 0$ , Equation (8) can be approximated as:

$$\omega_p \leqslant \omega \cdot (b-a)^{\frac{1}{p}}.$$

According to Lemma C.6 and satisfy the error limit  $\delta$ , s.t.  $E_n(f) \leq \delta$ , we have

$$\omega\left(f,\frac{1}{n}\right) \leqslant \frac{\delta}{12}.$$

To obtain the lower bound on n, since  $\omega(f, h)$  is a nondecreasing function with respect to h, we take its inverse function  $\omega^{-1}(f,y)$  as follows:

$$\frac{1}{n} \leqslant \omega^{-1} \left( f, \frac{\delta}{12} \right). \tag{9}$$

Finally, the lower bound for n can be derived from inequality (9) as:

$$n \geqslant \frac{1}{\omega^{-1}\left(f, \frac{\delta}{12}\right)}.$$

Lemma C.4 provides a minimum bound related to the value of the modulus of continuity. Furthermore, the Lipschitz continuity [135] of vehicle trajectories  $X_i$  and  $Y_i$  offers a more compact bound for inequality (7):

**Corollary C.7** *The bound in inequality* (7) *is satisfied as follows:* 

$$n \geqslant \frac{12L}{\delta},\tag{10}$$

where L represents Lipschitz constant.

The proof of Corollary C.7 consists of two parts: (i) establishing Lipschitz continuity of vehicle trajectories and (ii) deriving Equation (10).

#### (i) Lipschitz Continuity of Vehicle Trajectories

To demonstrate the Lipschitz continuity of vehicle trajectories, it suffices to show that their state information (Section 2.1), including (x, y) position, velocity v and acceleration a, satisfies the Lipschitz condition (L-condition). Specifically, there exists a constant L, s.t. for any  $x', x'' \in [a, b]$ , the following holds:

$$|f(x') - f(x'')| \le L|x' - x''|.$$
 (11)

According to the physical relationships among these states, if acceleration a satisfies L-condition, then by the boundedness theorem [136], the other states also satisfy it. Thus, we take a as an example, and similar arguments apply to the other states, quod erat demonstrandum.

According to [137, 138], the variation in vehicle acceleration is constrained by factors such as engine performance, vehicle weight, and braking system, which implies that the jerk j(t) (the rate of change of acceleration over time)

cannot be physically infinite. Therefore, there exists a constant  $M_j$ , s.t.  $|j(\tau)| \leq M_j$ . For any  $t_1, t_2 \in [a, b]$ , the following holds:

$$|a(t_1) - a(t_1)| = \left| \int_{t_2}^{t_1} j(\tau) \right| \le \int_{t_2}^{t_1} |j(\tau)|$$

$$\le \int_{t_2}^{t_1} M_j d\tau = M_j |t_1 - t_2|.$$

Therefore, Hence, the acceleration function a(t) is Lipschitz continuous with the Lipschitz constant  $L=M_j$ .

(ii) Derivation of a more compact bound.

To obtain a tighter bound, we use the L-continuity property of f. From the continues of modulus, we have:

$$\omega(f,h) \leqslant Lh \Rightarrow \omega^{-1}(f,y) \geqslant \frac{y}{L}.$$
 (12)

From Jackson's inequality in Lemma C.6, let  $y=\delta/12$  in Equation (12). This ensures that the error remains below  $\delta$ , with  $\delta/12$  acting as a piecewise error threshold. Then Equation (12) becomes:

$$\omega^{-1}(f,y) \sim \omega^{-1}(f,\frac{\delta}{12}) \leqslant \frac{\delta}{12L}.$$
(13)

Combining inequalities (7) and (13), we obtain the more compact bound (10).

#### C.3 Normal Drivers: Legendre Polynomial

In Section 3.2.3, we discuss that the speed and acceleration of normal drivers maintain an intermediate state between conservative and aggressive drivers. Their trajectories do not change as dramatically as aggressive drivers, nor are they so slow as to affect the flow of traffic. To approximate these trajectories, we use the Legendre polynomial  $L_n$ . The minimum degree n of  $L_n$  is obtain by:

**Theorem C.8** For all  $\epsilon > 0$ , if  $\partial [L_n(f)] = n$ , for a given error limit  $\delta$  with  $0 < \epsilon \le \delta \ll \infty$ , then

$$n \geqslant \left(\frac{C_H}{\delta}\right)^{1/\alpha},$$
 (14)

where  $C_H$  is Hölder constant modulus of continuity and  $\alpha$  represents Hölder exponent.

From Theorem C.8 we apply Jackson's inequality (Lemma C.6) to establish a relationship between the approximation and the modulus of continuity. This inequality also applies to continuous functions defined on the interval [-1,1] interval. To achieve the bound in Equation (14), we further use the Hölder continuous property [139] of vehicle trajectory. Similar to L-continues as defined in Equation (11), Hölder continuous (H-continuous) is define as follows:

**Definition C.9** (Hölder continuous) For a function f defines on interval I, if there exits a constant  $C \in \mathbb{R}$ , s.t. for  $\forall z'^{,z''} \in I$ :

$$|f(z') - f(z'')| \le C_H |z' - z''|^{\alpha}, \ \alpha \in (0, 1],$$

then f is is said to be Hölder continuous of order  $\alpha$ .

When  $\alpha=1$ , *H*-continuous reduces to *L*-continuous. Reference [140, 141, 142, 143] analyze the Hölder continuity or related smoothness of vehicle trajectories and their states (position, velocity, and acceleration), either directly or indirectly by examining the smoothness of physical constraints and changes. Therefore, the bound in Equation (14) can similarly be derived from inequality (12):

$$\omega(f,h) \leqslant C_H h^{\alpha} \Rightarrow C_H \left(\frac{1}{n}\right)^{\alpha} \leqslant \delta.$$

Thus, we obtain a bound as expressed by inequality (14).

#### **D** Effects of Framework Sensitive

In Section 4.3, we evaluate our DSA framework with respect to module component dimensions: namely the type, combination, and degree of polynomials  $p_n$ , as well as the driving style matching. In this section, we further analyze the sensitivity of our model with regard to: variations in the driving style categories themselves (Section D.1), external influences such as changing traffic densities (Section D.2) and varying road conditions (Section D.3).

#### D.1 Number of Driving Style

In reference [48, 49, 50] we know that driving style are categores as three type and each characters are illustrated in Section 3.2. Now we use automatic manner category numbers rather than the predefining for driving styles. Specifically, we evaluate multiple-category settings using K-means clustering, and report the corresponding metrics (log-normalized results except for Silhouette metric) on the Argoverse (from A- $\triangle$ WSS) and nuScenes (from N- $\triangle$ WSS) in Table 8, here for all metrics listed below, larger values indicate better clustering performance. Our three-category configuration yields the highest number of best scores across the metrics, supporting the

Table 8: Clustering evaluation results on Argoverse (A) and nuScenes (N). A value of "1" indicates the best performance among all settings.

k	$A-\Delta WSS$	Silhouette	$\Delta \text{CHI}$	N-∆WSS	Silhouette	$\Delta \text{CHI}$
2	-	0.919	-	-	0	-
3	1	1	0.810	1	0.700	1
4	0.743	0.986	1	0.586	1	0.387
5	0.022	0.283	0	0.287	0.268	0.324
6	0	0	0.601	0	0.398	0

validity and rationality of our chosen driving style taxonomy. The metrics [144] are defined as follows:

- WSS (Within-Cluster Sum of Squares): Measures the improvement in intra-cluster compactness. A
  higher value suggests tighter grouping of samples within clusters after clustering.
- Silhouette: Reflects both the cohesion within a cluster and the separation between clusters. A higher silhouette score indicates that samples are well matched to their own cluster and poorly matched to neighboring clusters.
- CHI (Calinski-Harabasz Index): Captures the variation in inter-cluster separability and intra-cluster compactness. Higher values indicate better-defined and more distinct clusters.

#### **D.2** Traffic Density

Traffic density is closely related to vehicle speed and traffic flow, and significantly influences trajectory prediction due to varying interaction patterns among vehicles [145]. To clearly present the impact of traffic density, we divide the dataset into five levels based on the number of vehicles per unit area. We compare the performance of our DSA framework against the best-performing baseline with publicly available code: Context-Aware [81], as identified in Table 1. The comparison results are illustrated in Figure 5.

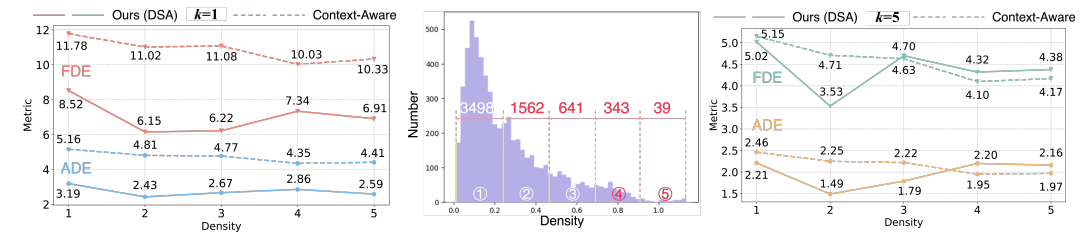


Figure 5: Comparison of trajectory prediction performance under different traffic densities with Context-Aware [81]. Our method is represented by solid lines, while Context-Aware is depicted using dashed lines on both sides. The middle subfigure shows the density distribution with circled numbers indicating the corresponding density levels.

Our DSA framework consistently outperforms the baseline across over 75% of the dataset. When averaged over the highest-density and most common case (density level 1 in the middle subfigure of Figure 5), our method achieves improvements of 1.97 in  $ADE_1$  and 3.26 in  $FDE_1$ , as well as 0.25 in  $ADE_5$  and 0.13 in  $FDE_5$ .

The most notable gains appear in density level 2, where DSA reduces prediction errors by 49.48% and 44.19% for k=1, and by 33.78% and 25.05% for k=5, compared to Context-Aware. Although our framework shows slightly lower performance in levels 4 and 5 when generating 5 trajectories, these cases together account for only 6.28% of the dataset.

#### **D.3** Road Condition

Road structure significantly influences the motion patterns of agents navigating through urban or highway environments and is thus essential for accurate trajectory prediction [146, 11, 112]. Does road complexity increase the frequency of driving style changes, thereby making prediction more difficult? To investigate this question, we evaluate the performance of our DSA framework under different road conditions, as shown in Table 9.

Table 9: The b-minFDE\* in different road condition on the nuScenes dataset. The **best** results are highlighted.

Method Type	Stationary	Straight	Straight right	Straight left	Right U-turn	Right-turn	Left U-turn	Left-turn	All
MTR [147]	2.15	2.58	<b>4.85</b>	4.26	8.13	4.82	<b>5.17</b> 5.28	<b>4.85</b>	2.86
DSA	<b>2.03</b>	<b>2.48</b>	4.96	<b>4.17</b>	<b>8.11</b>	<b>4.77</b>		4.87	<b>2.75</b>

<sup>\*</sup> Brier-minFDE (*b*-minFDE): bminFDE=minFDE+ $(1-p)^2$ , where p is the probability of probability of the best forecasting trajectory with minimum endpoint error (minFDE).

Our DSA framework achieves the lowest overall error of 2.75, improving upon the baseline by 3.85%. It outperforms the baseline in 6 out of 8 categories, including reductions in error for common scenarios such as Stationary (5.6%) and Straight (3.9%), as well as complex maneuvers like Straight-Left (2.1%), Right U-turn (0.25%), and Right Turn (1.0%).

Although MTR performs slightly better in Straight-Right and Left U-turn (by 0.11 in both cases), DSA matches or surpasses baseline performance in the most frequent and safety-critical trajectory types. These results demonstrate the robustness and adaptability of our framework across diverse road semantics, particularly in non-linear or discontinuous motion patterns.

#### E Detailed Description of the Algorithm

In Sections 3.3.1 and 3.3.2, we introduced the mechanisms for polynomial combination and degree adaptation. In this section, we provide a detailed description of the corresponding algorithms.

#### **E.1** Polynomial Combination

To match each trajectory under various driving styles to a suitable polynomial combination, as analyzed in Section 3.2, we employ a Mixture of Experts model based on Top-K Gating (MoE-TopK) [63]. In this method, tunable Gaussian noise is added to the gating logits, and only the top K values are retained for expert selection.

Let us denote by G(x) and  $E_j(x)$  the output of the gating network and the output of the j-th expert network for a given trajectory  $X_i$ , for clearly we omit subscript i. The output  $z^{\text{com}}$  of the MoE module can be written as follows:

$$z^{\text{com}} = \sum_{j=1}^{3} G(X)_{j} E_{j}(x).$$
 (15)

As shown in [21, 61, 62], kernel density estimation and latent variable analysis reveal that a driver's behavior evolves continuously across different situations. This implies that driving behavior can be viewed as a probabilistic mixture of weighted driving styles. Given that drivers may exhibit behaviors characteristic of multiple styles in dynamic scenes—such as when another agent suddenly appears—we adopt the Noisy Top-K Gating network [63] to capture this mixture behavior. This network activates only the top-k best-matching experts, enhancing responsiveness and specificity. Accordingly, this modification adjusts  $G_*(\cdot)$  in Equation (15) to G(x), detailed as follows:

$$\begin{split} \widetilde{G_{j}(x)} &= \operatorname{Softmax}\left\{\operatorname{KeepTopK}\left[H(X),k\right]\right\}, \text{with} \\ H(X) &= &(X \cdot W_{G_{j}}) + \operatorname{SN}\left() \cdot \operatorname{Sp}\left[\left(X \cdot W_{\operatorname{noise}_{j}}\right)\right]. \end{split}$$

Here, "SN" and "Sp" denote Standard Normal [64] and Softplus [65] functions, respectively. The symbol  $W_*$  denotes the weight matrix corresponding to each subscript. The loss function is defined as follows:

$$L_{\text{MoE-K}} = w_{\text{load}} \cdot \text{CV (loads)}^2, \tag{16}$$

where "load" refers to the importance values assigned to each driving style, with  $w_{\text{load}}$  representing the corresponding weight. "CV" stands for the Coefficient of Variation, which assesses the variability of these values. Equation (16) is a part of Loss in Section 4.1. This structure of the MoE model effectively recognizes the diversity of trajectories, allowing each expert to specialize in different features of driving styles.

#### E.2 Degree Adaptation

From Theorem 3.7, we understand that the accuracy of polynomial  $p_n$  approximation is directly influenced by the degree n of the  $p_n$ . However, adapting the degree of  $p_n$  poses a complex, non-convex, and combinatorial optimization challenge, as the relationship between prediction error and polynomial degree is not straightforward. This complexity often leads to the presence of multiple local optima.

To address this issue, we utilize the versatile Bayesian Optimization (BO) tool SMAC3 [66] for its robustness and flexibility, making it particularly suitable for optimizing low-dimensional and continuous functions (type: SMAC4BB), such as those found in vehicle trajectory prediction.

We treat the adaptive of polynomial degree as a hyperparameter optimization problem, using SMAC3 for BO, which leveraging Gaussian Processes with the Matérn kernel and the Expected Improvement acquisition function, iteratively searches the candidate degree set to minimize the loss function. Specifically, the degree n is treated as a hyperparameter optimization problem, aimed at minimizing the loss on validation data  $D_{\rm val}$  of our model trained on training data  $D_{\rm train}$ . This process can be formulated as follows:

$$n_{SMAC} \in \operatorname*{arg\ min}_{n \in \mathbb{Z}^{+}} c\left(n\right) = \operatorname*{arg\ min}_{n \in \mathbb{Z}^{+}} L\left(\mathcal{D}_{train}, \mathcal{D}_{val}; n\right),$$

The hyperparameter optimization process targets the degree  $n_{\text{SMAC}}$ , which is defined as the optimal degree that achieves the least error for the corresponding basis function  $p_n$ . Here L denotes the loss function.

#### F Limitation and Discussion

**Limitation** We summarize existing open vehicle trajectory prediction datasets in Table 10, and observe that the maximum available trajectory duration is typically less than 10 seconds. Despite this limited time span, our framework based on three driving styles adapts well to such settings. We evaluate its performance on both short-term (3 seconds, Table 1) and long-term (8 seconds, Table 2) prediction tasks, achieving consistently strong or state-of-the-art results across all durations.

Table 10: Existing vehicle trajectory datasets. "His" and "Pre" represent the historical and predicted trajectory durations, respectively, while "Total" denotes the overall duration for each vehicle.

Datasets	Pub.	Collect Locations		Pre	Total
KITTI [148]	2012 CVPR	Karlsruhe	2	4	6
Apolloscapes [149]	2018 CVPR	Beijing, ShangHai and SHenZhen	3	3	6
nuScenes [67]	2020 CVPR	Boston and Singapore	2	6	8
Argoverse [68]	2019 CVPR	Miami and Pittsburgh	2	3	5
INTERACTION [150]	2019 arXiv	China, Germany and Bulgaria	1	3	4
InD [151]	2020 TIV	German	3.2	4.8	8
RounD [152]	2020 ITSC	Aachen	2	4	6
HighD [153]	2018 ITSC	German	2.8	2.8	5.6
Waymo [69]	2020 CVPR	USA	1	8	9

However, in longer prediction horizons, the complexity of driving behavior increases, suggesting that three driving style categories may be insufficient to cover all possible scenarios. Moreover, trajectory patterns are often influenced by external factors, which can be categorized as either soft or strong conditions.

Soft conditions, such as weather, affect driver perception and reaction. For example, on sunny days, improved visibility may enhance drivers' responsiveness, leading to smoother and more stable trajectories. In contrast, adverse weather conditions such as fog, heavy rain, or snow can result in more abrupt or irregular driving behavior.

Similarly, strong conditions such as traffic signals or regulatory constraints also significantly influence vehicle trajectories. Unfortunately, most existing datasets lack labels for these contextual factors. We believe that incorporating such labels could further enhance prediction accuracy in future research.

**Discussion** For longer vehicle trajectories, we can improve our DSA framework from both practical and theoretical perspectives.

- Incorporating more driving styles. Our current DSA framework utilizes three representative styles:
   Conservative, Aggressive and Normal (CAN), which reflect two behavioral extremes and an intermediate pattern. However, as the temporal length of each driver's trajectory increases, driving behaviors may exhibit greater variability. To capture these nuances, the model can be extended by defining or integrating additional driving styles. This would allow for a more fine-grained characterization of driver behavior and potentially lead to improved trajectory prediction accuracy.
- 2. Expanding the set of basis functions. As driving styles become more diverse and trajectory conditions more complex, a broader set of basis functions is required to effectively approximate and predict vehicle trajectories. Instead of relying on a single polynomial type, we can extend to a set of basis functions of the same class, such as orthogonal trigonometric polynomials. For example, to minimize the L² norm in modeling trajectories of normal drivers, or other intermediate states between conservative and aggressive behavior. It is beneficial to use a richer set of orthogonal polynomials that better match the dynamics of these nuanced driving styles.

#### **G** Future Work

In this paper, we focus on the characteristics of the individuals who generate the data (i.e., trajectories) and leverage the mathematical properties of basis functions to approximate these trajectories. This concept can be generalized and extended to other domains, such as:

- Other traffic participants. In addition to drivers, other agents in the traffic scene such as pedestrians and cyclists, also exhibit distinct behavioral characteristics. By modeling these characteristics, we can select appropriate basis functions tailored to each agent type, thereby improving the accuracy of their trajectory prediction.
- Multivariety Time Series Forecasting. Our framework can be extended to long-term forecasting tasks
  in domains such as weather prediction, energy consumption and electrocardiography. For example,
  one could model temperature and precipitation trends across different climate zones, analyze electricity
  usage patterns based on consumer behavior, or study heart rate dynamics as a function of individual
  health conditions.

Additionally, by leveraging the core theoretical foundation (Theorem 2.2), we aim to construct models grounded in the physical characteristics or behavioral attributes of the data sources, thereby fully exploiting the inherent structure of the data itself.

#### **H** Visualization

Due to space constraints, the number of visualized prediction results in the main text is limited. Here, we provide additional visualizations of predicted trajectories for various scenes, with generated trajectories k=1,5,10. Each value of k is presented for both simple (e.g., straight roads) and complex scenes (e.g., turns conditions), showcasing different types of driving behavior.

To enhance the clarity of the visualization results, we present them on a dedicated page and reduce the background opacity to improve visual contrast. Specific outcomes are accompanied by detailed explanations provided in the corresponding figure captions. In summary, considering various scenario combinations and adjusting the number of generated trajectories lead to more diverse, accurate, and comprehensive vehicle trajectory predictions. Increasing the number of predicted trajectories improves prediction diversity and realism, while analyzing different scenarios helps adapt to the diversity and complexity of real-world traffic environments. These improvements contribute to making the model both more mathematically grounded and more adaptive.



